Gonzalez

Nuclear Engineering and Design 66 (1981) 301–332
North-Holland Publishing Company

AN ASSESSMENT OF CLASS-9 (CORE-MELT) ACCIDENTS FOR PWR DRY-CONTAINMENT SYSTEMS *

T.G. THEOFANOUS and M. SAITO

School of Nuclear Engineering, Purdue University, West Lafayette, IN 47907, USA

Received 27 July 1981

The phenomenology of core-melt accidents in dry containments was examined for the purpose of identifying the margins of safety in such Class-9 situations.

The scale (geometry) effects appear to crucially limit the extent (severity) of steam explosions. This together with the established reduced explosivity of the corium-A/water system, and the inherently high capability of dry containments (reinforced concrete, and shields in some cases, seismic design etc.) lead to the conclusion that failure due to steam explosions may be considered essentially incredible. These 'premixture' scaling considerations also impact ultimate debris disposition and coolability and need additional development.

A water-flooded reactor cavity would have beneficial effects in limiting (but not necessarily eliminating) melt-concrete interactions. Independently of the initial degree of quenching and/or scale of fragmentation, mechanisms exist that drive the system towards ultimate stability (coolability). Additional studies, with intermediate-scale prototypic materials are recommended to better explore these mechanisms.

Containment heat removal systems must provide the crucial capability of mitigating such accidents. Passive systems should be explored and assessed against currently available and/or improved active systems taking into account the rather loose time constraints required for activation.

It appears that containment margins for accommodating the hydrogen problem are limited. This problem appears to stand out not only in terms of potential consequences but also in terms of lack of any readily available and clear cut solutions at this time.

1. Introduction

Realistic understanding of core-melt accidents and their consequences in Light Water Power Reactors is important for the comprehensive determination of *Risk*. Such determinations would be a crucial factor in the current debate concerning long term Nuclear Power policy. Perhaps more importantly, however, such understanding is essential for *optimizing resources* with respect to minimizing the risk through a balanced approach in pursuing Research and Development and implementing safety features addressing the whole spectrum of off-normal operation.

The impetus for understanding Class-9 accidents as well as the current state of the art in this area are best exemplified with the work surrounding the so-called ZIP (Zion/Indian Point) Study. A wide range of relevant theoretical and experimental information has been brought forth especially as a basis for the extensive mechanistic calculations carried out with computer codes (MARCH, SIMMER, etc.). These studies are helpful in providing a general-purpose parametric feel for the various effects and their significance. They may not represent the best approach however insofar as providing the comprehensive perspective required for arriving at conclusions. The basic reason for this is that many more degrees of freedom, concerning qualitative phenomena as well as their quantitative features, than those practically realizable by means of large scale computations, are needed to account for stochastic behavior as well as for limitations in the mathematical modeling (including input-speficied data) of such a complex set of phenomena. At the other extreme probablistic risk assessment studies do not contain the mechanistic insight required. It is suggested then, especially when specific concerns (i.e., the steam explosion or core–concrete interaction hazards) are to be addressed, that a more generic phenomenological structure may provide an appropriate

* This work was performed under the auspices of the United States Nuclear Regulatory Commission, Washington, D.C. 20555 under contract No. NRC-03-80-102.

0029-5493/81 0000–0000/$02.75

approach. An attempt in this direction is made here. There are two specific phenomenological aspects of this problem, not considered previously, that possess such generic character and have prompted us in this path of investigation. We introduce them briefly below.

1.1. Effect of scale on fuel-coolant mixing

Mixing between two liquids is an interface phenomenon. For macroscopic systems (much greater than the stable droplet size) the surface to volume ratio decreases with size, and for the same contact time (distance of travel), the relative proportions of masses found in intermixed states will also diminish. This consideration is crucial not only in assessing the likelihood of a major steam explosion (i.e., involving a significant fraction of the fuel inventory) but also in developing a realistic view of resulting fuel debris configuration and hence coolability. The relevant fuel volumes are nearly three to four orders of magnitude larger than the largest available (and practically reasonable) experiments. In addition, the available experiments have utilized an overabundance of coolant. The geometric scales, and contact length scale in particular are thus grossly distorted in the direction of favoring intermixing, explosions, and/or fragmentation. Such is the case, for example in the EXO-FITS experiments. Yet Berman et al. [2] concluded that fuel mixing occurs quickly and at a fine scale (< 1–2 cm) even for the reactor application. We illustrate these phenomena experimentally and conclude that mixtures involving more than 2 and 10% of the fuel mass for in-vessel and ex-vessel explosions respectively are unlikely.

1.2. Effects of debris bed stability on coolability

For deep beds, as those of interest here, dryout is hydrodynamically controlled by the flow resistance (including counter-current flow limitations) within the bed. Dryout heat fluxes are therefore dependent upon particle sizes (i.e., void space sizes) increasing with particle size. Correspondingly, for any particular decay power level and debri bed height there is a particle size (less than 0.1 cm for our case) below which dryout would occur. To completely exclude such fragmentation although intuitively reasonable it represents an impossible task. We can, however, render the question amenable to a more definitive answer by considering instead the stability of all possible coolant–debri–concrete configurations and by showing that unstable beds (non-coolable) are driven to stability (coolable) by a spontaneous change in particle dimensions. Again the relevant phenomena are illustrated experimentally and it is shown that even prototypic material verification is feasible. The presence of coolant is key in these considerations. In contrast, current work (i.e., see reports during the November 1980 Core Melt Information Exchange Meeting held in Germany) is focused on corium–concrete interactions. Extensive computer code development has been underway for some time and super large scale (by current standards) interaction experiments, 600 kg melt and 5000–10000 kg concrete, have been planned for the next 1–2 years.

The general accident sequence (pressurized water reactors and dry containments are only considered here), especially as characterized by the amounts of materials interacting is discussed in section 2. Against this overall framework the concerns of Steam Explosion and Debri Bed Coolability are assessed in sections 3 and 4 respectively. Finally the containment pressure transient is estimated in section 5. A summary of conclusions is given in section 6.

2. Meltdown sequences

2.1. Generic geometric considerations and definitions

A scaled representation of the reactor vessel (and the internals important to the accident sequence) as situated in the reactor cavity is shown in fig. 1. A plan view of the reactor cavity and keyway is presented in fig. 2. Important volumes, areas, and dimensions are also noted on these figures. According to the findings of this report the presence of water is beneficial and a flooded reactor cavity is assumed throughout.

At decay heat levels the meltdown process is rather slow. *It would progress from within to the outside of the core forming a contiguous melt region.* A continuous melting and refreezing cycle would commence due to small passages available for melt escape and the substantial heat capacity in the lower portions of the core and its supporting structures. The molten zone would have to be contained by frozen crusts due to boundary losses. The melting–freezing process renders such crusts in a state of motion in the outward direction. Quite clearly the possibility of any amount of water present within this growing molten zone must be excluded. Also in view of the preferred downward fuel relocation the rate of growth in the downward direction will exceed that in the lateral (radial) direction. This virtual continuum of melt configurations (states) is likely to be interrupted each time a massive obstacle (core support structures) is encountered. Although the discreteness of

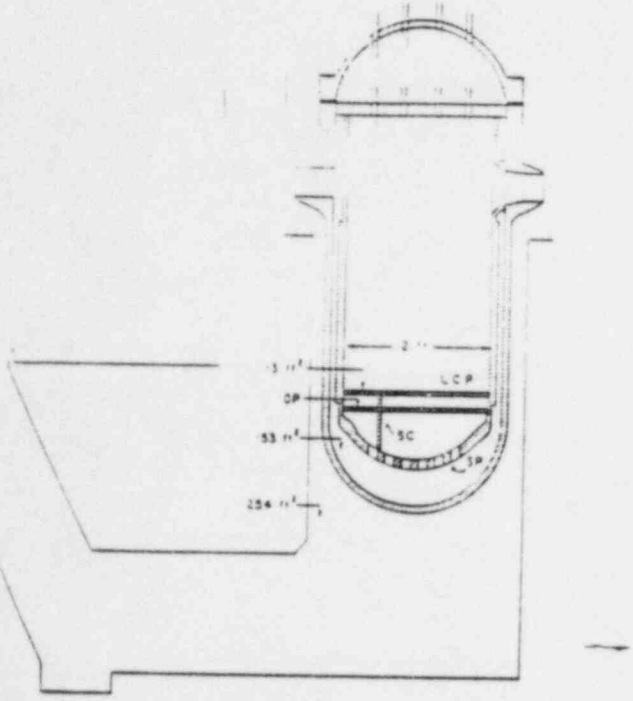

Fig. 1. Scaled representation of the reactor vessel situated within the reactor cavity. LCP-Lower Cover Plate, DP-Diffuser Plate, SC-Support Columns, SP-Support Plate.

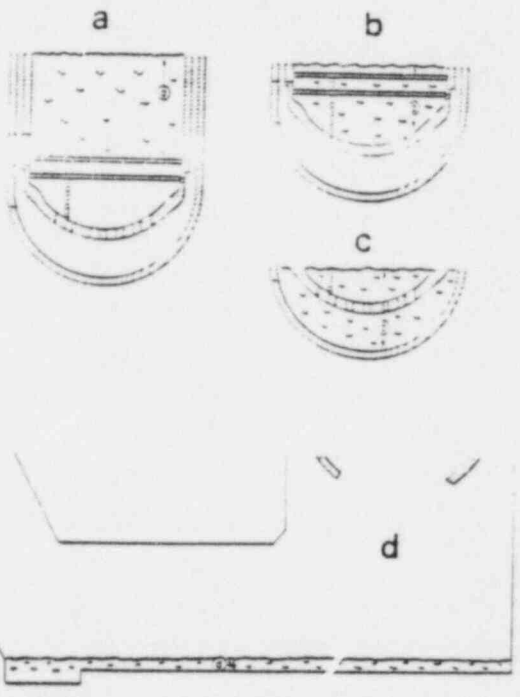

Fig. 3. Illustration of key molten fuel pool configurations (states).

these states may not be always very pronounced they are convenient milestones for the purpose of following the accident progression.

Three such states are identified for the in-vessel portion of the sequence. They correspond to the lower melt boundary coinciding with the lower core and diffuser plates, the core support plate, and the reactor vessel lower dome, and will be referred as states A, B, and C respectively. These states are schematically depicted in fig. 3. Prior to penetrating the lower core and diffuser plates the pool would contain at most 400 ft^3 of melt. A more likely figure would be one-half as much. Upon reaching state A the radial growth may exceed the downward relocation. States B and C would hence occupy volumes closer to the maximum values of 450 and 500 ft^3 of melt respectively. The final state, state D, corresponds to melt capture by the reactor cavity floor and it is amenable to a number of possible configurations. The most likely, an even distribution of essentially the whole amount of melt over all available reactor cavity area, is designated as state D. Finally the possibility of dispersing some of the debri outside the reactor cavity (in the containment) by fuel-coolant interactions (or other pressure releasing events) need be considered for completeness. This possibility will be discussed later, however, as we will see the uncertainties associated with the dispersion of major quantities are such that it would not appear prudent to generically take direct credit for this mechanism. Hence no specific state will be defined. In as much as any amount of dispersal will reduce the heat load on the reactor cavity, however, this will be a factor added to a long list of other favorable, yet unquantifiable, mechanisms viewed as providing additional margins to safety.

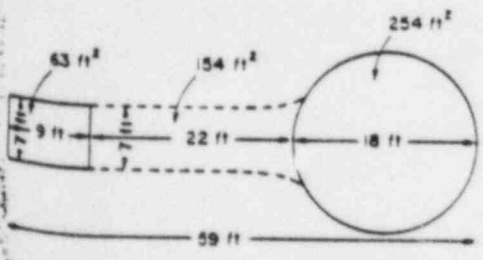

Fig. 2. Plan view and typical dimensions of reactor cavity and keyway.

In considering the long term behavior of the stability

of each one of these states with respect to interactions of the melt with the various materials with which it comes in contact, i.e., structural components identified as supporting elements for each state, must be assessed. The possible influence of the presence of coolant, and associated fuel/coolant thermal interactions need also be considered.

In the past (i.e., WASH-1400) the likelihood of an energetic, large-scale (~20% of core), interaction, was estimated as "one out of ten times" that a "large molten mass" encounters water. Such encounters during a core-melt accident were taken as virtually certain (probability of unity). More recently, and on the basis of certain "prototypic material" experiments at Sandia, it has been recommended that any one encounter (again taken as certain) of the molten core with a quantity of coolant (i.e., damping of the ECCS accumulators) would produce an energetic, large scale, fuel–coolant interaction, known as vapor explosion (i.e., an upwards adjustment of the probability by a factor of 10). Even more recently (Berman et al. [2] this probability was reduced by a factor of 2. What is implicit in these estimates is that every 'encounter' and every explosion would involve substantial fractions of the available melt. On this aspect of the problem we would like to give our primary consideration.

It has been widely recognized for some time now, that coherent, large scale, explosions, involve the triggering and propagation processes through a fuel–coolant mixture (to be referred to here simply as 'premixture') that is coarse enough to allow essential thermal isolation between fuel and coolant, yet it is fine enough to support the process of propagation. The actually required range of 'scales' of this premixture is not known to date. It does appear, however, that from the point of view of actual participation in the heat exchange process, for the time scales, pressures, and velocities of interest a 10 cm scale should be an adequate upper bound. The adoption of such length scale now provides a handle to explicitly account for scale and geometry effects in carrying out order-of-magnitude estimates (as given in the subsequent two sections) of the potential extent of fuel-coolant interactions at the various stages of the meltdown sequence. The amount of coolant in a premixture should be of the same order as that of the fuel. Such a potentially explosive premixture involving mass m^f and m^c of fuel and coolant respectively will be denoted by $m^f \cup m^c$ (the mathematical symbol for the 'union' of sets). Based on the above, from the point of view of energetic interactions, the meltdown sequence may be characterized by the probability for a premixture as a function of the quantities involved and time, i.e., $P(m^f \cup m^c, t)$.

We will find that due to the particular geometric constraints 'premixtures' are of limited extent and short lived. The most likely times for their occurrence will be during transitions between states. It is more convenient, therefore, and certainly more pertinent to the degree of actual knowledge implied, that the premixture probabilities be referred to a certain instant in time (presumably the one maximizing its value). The continuous functionality in time will, therefore, be removed in favor of indicating the time period by the corresponding melt configuration state, as defined above, i.e., $P_B(m^f \cup m^c)$ meaning the probability for a premixture, able to support propagation involving a quantity of fuel mass m^f and occurring within the geometrical confines of state B, during or just after the transition A → B. Crude estimates of these premixture probabilities are given in the subsequent two sections. The main intent is to argue, on physical grounds, for the existence of cutoff points (bounds), and to provide some judgment as to whether these bounds are approached gradually or abruptly. The graphical presentation of continuous distributions is provided on these bases and should not be taken to imply anything more quantitative than that.

2.2. *In-vessel states and their transitions*

During the pool growth phase of state A water may be encountered either by reaching existing quantities remaining at lower elevations or due to belated addition of emergency water. As it is to be noted throughout this study the presence of water at any stage can only have beneficial effects. In the case of state A continuous availability of plentiful water, especially through the downcomer *may even stabilize* the accident at this point. *Such early and continuous availability of water would be worth the most serious considerations in any effort extending the engineered safety features into the so-called degraded core cooling area.*

On the other hand, for the purposes of current assessments we must consider the eventuality of water availability rather late into the meltdown process. On the basis of the contiguous geometry of phase A and the fuel and coolant densities, we are unable to identify a mechanism leading to 'premixtures' at this stage. This conclusion is independent of accident and mode of water injection. This is shown in fig. 4 by the rapid fall-off of the probability $P_A(m^f \cup m^c)$ [illegible] mark taken as the upper limit for a totally segregated system (i.e., the characteristic dimension of the mixture is that of the whole melt). Exactly the same arguments and conclusions are pertinent also to states B and C.

...ization, on the other hand, in states B and C ... be considered progressively less likely (but not ... impossible) compared to that in state A. In ... from above, stabilization in either state B or ... would require substantial cooling from below. For ... counter-current flow limitations may become ... while external and effective insulation re... submerging of the reactor vessel (state C) ap... *incolute* rather than significantly improve the ... Clearly, however, availability of downcomer water below state B is desirable since even if it is unable to ...ilize it will certainly delay transition to state C.

The transition A → B due to the presence of support ...ms will most likely be gradual. The transition ... could be gradual but it may also follow the ...astrophic failure of the core support plate along its ...tact with the core barrel. In both cases, however, the phenomenology is crucially affected by the small dimensions of the receiving volume relative to the melt dimensions (see figs. 1 and 3). In a catastrophic failure for example of the core support plate the plenum water (if any) will be pushed out (by the solid support dome) into the downcomer regions rather than mix with the melt. Again the characteristic dimension will be that of the whole melt, and the probabilities will fall off rapidly around the 1% mark. This behavior is illustrated by the $P_{A\to B}$ and $P_{B\to C}$ in the 'fast' transition cases shown in fig. 4. Now let us consider an arbitrary pour ('slow' transitions) from a melt-through path of dimension d_j. Due to the short fall distances involved (2–3 ft) negligible jet breakup would be expected (see Appendix A). The melt would begin to accumulate at the bottom displacing water into the downcomer region. For pours under such conditions triggering may not take place at all, but if it did it would most likely occur at the initial impact of the jet with the wall, i.e., early in the pour process. In any case, however, at any instant in time the 'premixture' may not involve quantities larger than one jet length. For jet diameters up to the approximate maximum premixture dimension (~ 10 cm) the quantity of fuel would be 0.3 ft^3. Even for the unlikely large diameter of 3 ft, and an unrealistically high surface depth mixing of ~ 10 cm, a fuel quantity of ~ 10 ft^3 is estimated. This corresponds to ~ 2–3% premixture and the probability trend is illustrated in fig. 4. Up to the value of 3% the fall-off in probability is given as gradual due to uncertainties in the mixing process and the intent to provide reasonably bounding estimates. A very rapid fall-off however is appropriate within the 3–4% range.

For the in-vessel portion of the melt sequence the conclusion is that even in the presence of water (which is anyway desirable) any large scale premixing (or even quenching) would be essentially impossible. To fully prove this impossibility would not appear practical. However, the matter does not entirely belong with those euphemistically referred to as "engineering judgment." Instead it represents a fundamental 'scaling' question and at this time such scaling trends are easily observed even in small scale experiments as discussed in Appendix A.

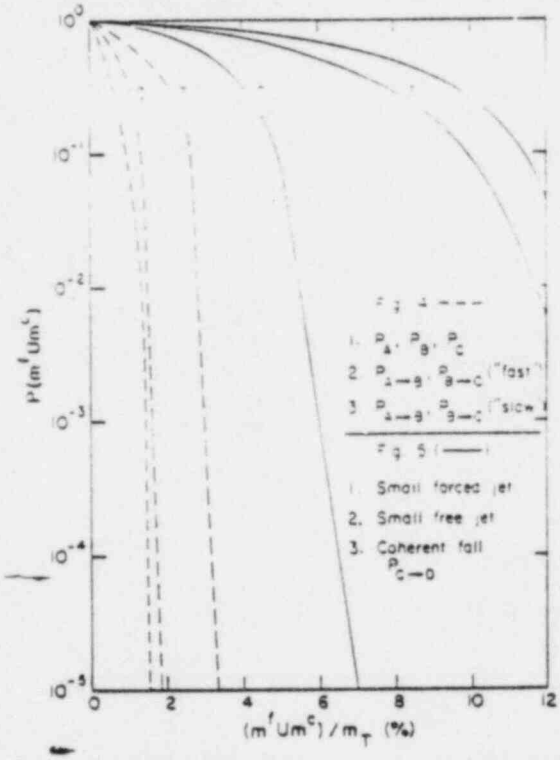

Fig. 4. Premixture probabilities for in-vessel states and transitions as function of the fuel masses involved.

Fig. 5. Premixture probabilities for ex-vessel states and transitions as function of the fuel masses involved.

2.3. Ex-vessel states and transitions

The discussion here parallels that of the previous section and again is based on Appendix A. With reference to fig. 1 the geometry here is somewhat more favorable (than the in-vessel situations) to 'premixing,' however, it is still far from what would be required to expect premixing at large scale. Again, the water depth is very limited and the fall distance amounts to slightly over twice the melt's own characteristic dimension. Fur-

ther, due to large density difference the fuel and water would tend to quickly stratify, i.e., any premixtures would be highly dynamic and short-lived. Again we distinguish between a 'slow' jet-like pour and a 'fast' fall due to catastrophic failure of the lower reactor vessel dome to estimate P_{C-D}.

A 'slow' event would most likely involve a pressurized primary system and a local vessel failure. Such failures would tend to break up the fuel jet as it leaves the reactor vessel at high velocity and would hence be most favorable for the production of 'premixtures.' However, such failures would be also most likely to occur near the top of the melt (where heat transfer to the boundaries is a maximum due to the natural convection pattern) by the combination of thermal and mechanical stresses. Hence a rather small quantity of fuel would be available for this forced jetting. The internal pressures would quickly fall off and the remaining fuel would most likely rest until a subsequent catastrophic failure and a 'fast' coherent fall. Even less amount of 'premixture' would be expected in the case of a 'free' (gravity driven) jet. Based on the discussion of Appendix A we do not expect breakup for jets with larger than 1 ft diameter, i.e., for 5 ft submergence we estimate ~ 1% premixture. For larger jets the surface entrainment would be self-limiting. Assuming an arbitrarily large boundary layer (on the jet surface) of 15 cm and a 3 ft jet yields premixtures of ~ 5%. For the forced jet and for a likely breech within the upper 1 ft layer of melt about 20% of the mass could be expelled. About half of this mass is taken as a bound for the premixture. These physical situations are depicted in fig. 6 and the corresponding probabilities are shown in fig. 5. A half-full cavity was assumed in these estimates. An adjustment by a factor of 2 would be required for a completely full cavity.

A 'fast' event most likely would involve the catastrophic failure of the lower dome through weakening of the wall around the periphery as shown in fig. 7. A low pressure primary system would favor this event. A coherent fall as shown in fig. 7 and rather minimal premixture formation is envisioned under these circumstances. Even if the whole lower dome was assumed to be very weak and near failure at this point neither the forces nor the mixing (travel) times are present to promote the formation of 'premixtures.' The upper 1–2 ft as shown in fig. 7 would appear an upper credible [illegible] curve is shown in fig. 8.

For the ex-vessel portion of the melt sequence we conclude that although the premixture quantities potentially present are one order of magnitude greater than those envisioned during in-vessel sequences, still, they cannot be reasonably expected to exceed 10% of the core inventory. Further it appears that even quenching of the major portion of the melt would be limited in most cases by the high degree of fuel segregation expected (see Appendix A). Continuation of this discussion from the point of view of debris quenching and coolability is resumed in section 4.

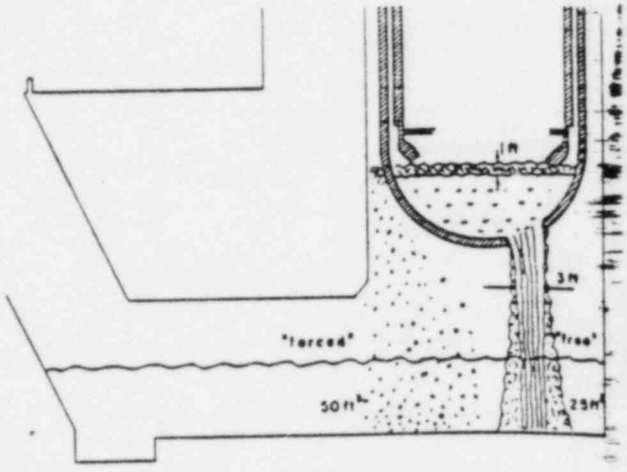

Fig. 6. Illustration of premixture concepts likely to develop from local lower dome failures.

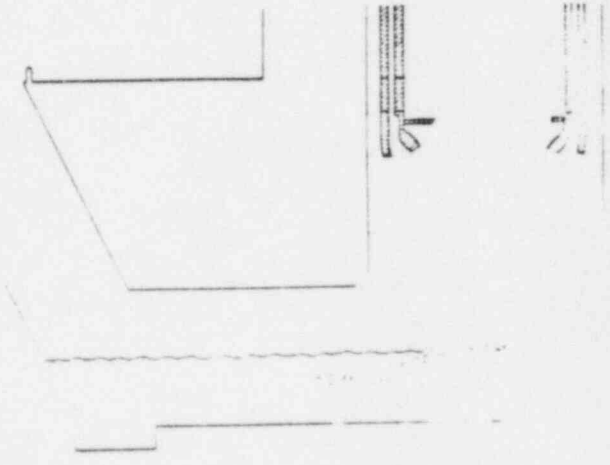

Fig. 7. Illustration of premixture concepts likely to develop from catastrophic circumferential lower dome failure.

3. The steam explosion concern

3.1. The concern and the approach

The molten core at around the fuel melting [illegible] MJ of thermal energy is potentially available. Conversion of this thermal energy, coherently, into mechanical work could represent a significant challenge to the containment. However, as we have already discussed in the previous chapter only a small proportion of the molten fuel mass would be expected to participate in a coherent interaction. Even with those small amount of interacting fuel, thermal energies of the order of 4000–20000 MJ need be considered for in-vessel and ex-vessel respectively (taken at 2% and 10% respectively). At thermodynamically ideal conversions (~30%) they would represent releases of 1200–6000 MJ (based on expansion to one atmosphere). However, the actual manifestation of such releases would require an adequate inertia constraint as well as the coincidence between the bounding quantities of 'premixture' estimated and the triggering and the sustained propagation of the explosion. Furthermore, nonideal efficiencies, due to the rate processes during the propagation and early expansion phase, as well as to condensation losses during the early expansion phase (acceleration) would tend to reduce the actually attainable releases. These considerations need finally be related to the potential for containment damage.

3.2. Steam explosion fundamentals

The molten debris/water system is well within the film boiling range. As such it favors the attainment of good premixtures *provided* that also favorable geometric and pouring conditions exist. Thus the premixture quantity (extent) may be increased by dropping a fuel jet already in the state of breaking up (i.e., allow dropping elevation or forced jetting from a nozzle) in a deep water container. Propagation involves the coupling between an advancing (into the premixture) pressure wave front, and the fast fuel breakup and intermixing with the surrounding coolant in the vicinity of the front. This extensive fragmentation is a necessary requirement for the occurrence of the explosion since it provides for the surface area yielding the enormous heat transfer rates. Several mechnisms have been proposed in the literature, prominent among them are one based on hydrodynamic (differential velocity) instabilities and the other on rapid boiling-induced instabilities. While both of them have been observed in special purpose experiments the connection of the explosion process to any one mechanism has not been clearly made as yet. Similarly we are even further away from knowing which are the *important* premixture characteristics and how propagation and efficiency are related to them. However, qualitatively at least the following trends, in our case, trends.

'Premixtures' (in film boiling) may be triggered into explosions spontaneously or by means of an externally applied sharp pressure pulse. The required external trigger amplitude (energy) seems to increase with pressure level, presence of noncondensibles in the vapor blanket, and increases of fuel temperature beyond the minimum film boiling temperature. Since all these trends may be connected to increased stability of the film boiling process, vapor blanket collapse seems to be well connected to the initiation if not also to the propagation phases. This is consistent also with trends observed in spontaneous explosions in the free pouring mode. Here, as the fuel temperature increases, a maximum in the 'likelihood' and 'violence' of the explosions is first observed, while these trends continuously diminish with further increases in the fuel temperature. In this connection the fuel freezing point is also relevant. If blanket collapse occurs well beyond the buildup of a surface crust, fragmentation (and explosion) would be rather unlikely. Since the film boiling process is connected to the coolant critical temperature (in a variety of possible ways, depending on a variety of available models, but such details are immaterial in the discussion here) a good measure of 'nonexplosivity,' defined as resistance to triggers from a film boiling condition, may be given by the temperature difference between the freezing point of fuel and the critical point of coolant, $\Delta T = T_f^f - T_c^c$. For the fuel/water system we have $\Delta T \sim 2000$ K while for the steel/water system $\Delta T \sim 1000$ K. This measure indeed agrees with observation in that the former system is rather difficult to trigger while the latter is known to explode spontaneously. From this point of view, the rather neglected simulant pair of water/liquid-N_2 appears to be much closer to the fuel–water system than many of the molten metal/water combinations utilized in simulations. The water freezes well above the critical temperature of nitrogen ($\Delta T \sim 150$°C) and the system has been difficult, albeit possible, to trigger into an explosion (Anderson and Armstrong, [1]). We have worked extensively with this pair in many different experiments (contacting modes) presented in this report, but we never witnessed an explosion.

A number of experimental studies with UO_2 and water, including in-pile power burst tests, reveal a rather benign interaction resulting to large smooth surface fragments typical of those expected from freezing at

film boiling. Recent tests at Sandia, Buxton et al. [3], utilizing 'large' amounts of corium A + R (~5 kg) and trigger pulses as high as 100 bar have failed to produce but one mild 'explosion.' Also Nelson's [6] experiments (15 g scale) demonstrate that in an appropriate geometry, and trigger, yielding explosions with reactor materials, the corium-A/water system proves nonexplosive. All details are not completely understood yet, and in the absence of information of premixture characteristics the full implications from the 'large-scale' Sandia experiments remain to be determined. However, it does appear that rather stringent premixture conditions and very energetic triggers are required to achieve large scale explosions with prototypic materials. With reference to the phenomenology outlined in sections 2.2 and 2.3 we can identify substantial trigger pulses only in connection with transition C → D (catastrophic failure of lower reactor vessel dome). However, in this case the trigger (impact of the whole plenum with the reactor cavity water and floor) would come well before the attainment of the 'premixture' state produced from the subsequent pouring of the plenum contents. Although the probability of an adequate trigger associated with the premixture probabilities of figs. 4 and 5 is judged as essentially zero a value of 10^{-2} and 10^{-1} for the in-vessel and ex-vessel contact states respectively will be adopted to reflect remaining uncertainties due to lack of fundamental understanding in premixture and trigger requirements for self-sustaining explosions. The one order of magnitude differentiation between these two probabilities is used to reflect melt composition differences with the in-vessel being more Corium-A like and the ex-vessel more Corium-E like (more metallic).

3.3. Estimation of mechanical energy release

Very little information is available concerning the efficiency of vapor explosions. The recent large-scale (up to 18 kg melt) Sandia experiments with Fe-Al_2O_3/water system indicate (Buxton and Benedick [3]) a conversion ratio (mechanical-to-thermal) of up to ~0.5%, while for those Corium A + R Water tests (up to 19.4 kg melt) for which *mild* explosion was observed a ratio of one order of magnitude smaller (0.05%) is reported [3]. Even for the Fe-Al_2O_3 case the ratio implies an efficiency (mechanical energy release to the maximum thermodynamically possible) of only ~1.5%. According to the estimates of section 3.1 such efficiencies would imply release of 18–90 MJ, i.e., an energetically negligible range.

However, the direct applicability of these experimental results must be viewed cautiously. As a result of the grossly distorted geometric scale and overabundance of coolant, i.e., fuel-to-coolant volume ratios of 1:500 to 1:1800, these tests would tend to magnify losses (condensation). Even more importantly, the actual amount of fuel found in 'premixture' and actually participating in the interaction (propagation) is not known. Hence the conversion ratio is estimated on the basis of the total fuel available obviously producing an underestimated efficiency estimate. Obviously these tests would produce very different premixtures than those expected in reactor conditions on account of an over four orders-of-magnitude variation in melt volume scale (surface to volume effect) as well as nearly two orders-of-magnitude distortion in mixing travel provided (see Appendix A). As a consequence these efficiency results cannot be interpreted as already incorporating the premixing efficiency expected in the application of interest.

Efficiencies of unity (thermodynamic limit conversions) have been deduced for some (with molten metals) industrial accidents. On the other hand, due to low value of the fuel thermal diffusivity we could not reasonably expect ideal conversions here. We would expect that the efficiency will also be a strong function of the 'premixture' conditions such as 'scale,' temperatures and constraints. The available theoretical understanding slowly progresses towards the goal of fully evaluating such details. Ultimately we believe it will be possible to demonstrate a best estimate value of ~10%. At this time however assuming a value less than 50% would be rather difficult to support. With this value we estimate 600 and 3000 KJ for the 2% and 10% interactions taken for the in-vessel and ex-vessel cases under consideration. Note that these estimates are based on expansions to one atmosphere and are used as indicative of the severety of the explosion. In reality only a fraction is available for contained geometries (in-vessel) or up to constraint breakthrough (ex-vessel). In a more detailed fashion we may express the probability to release a mechanical energy corresponding to the thermal [illegible] of fuel mass m^f (according to the previously discussed prescription) thus

$$P(E(m^f)) = P(I; m^f \cup m^c) P(m^f \cup m^c),$$

i.e., as the product to achieve a 'premixture' of [illegible] m^f times the conditional probability for the [illegible] of a trigger of the required amplitude [illegible] for the premixture [illegible]

figs. 4 and 5 and the trigger probabilities [illegible] section 3.2 the general behavior shown in fig. 3 [illegible] projected.

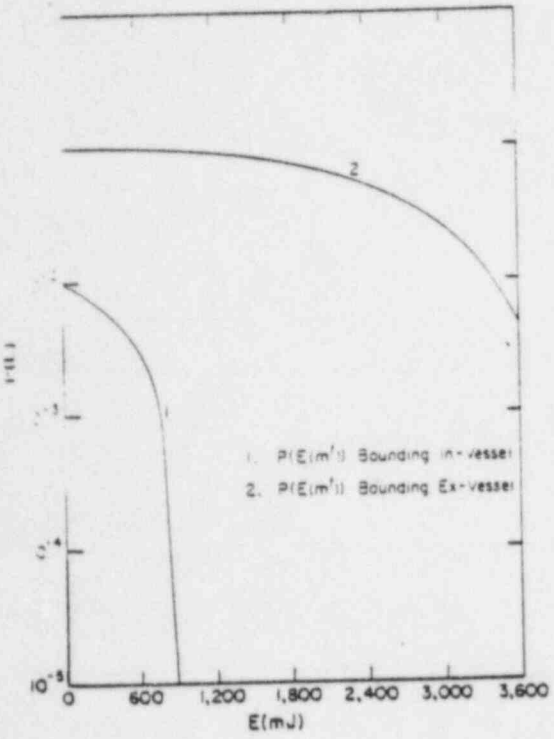

Fig. 8. Bounding estimates for the probability distribution of mechanical energy releases due to steam explosions.

3.4. The damage potential

No significant inertia constraints nor mechanisms for substantial missile generation may be identified for the ex-vessel explosion case. The rather large amount of energy involved would manifest as kinetic energy of the explosion fluids distributed equally in all directions. From the point of view of potential damage this explosion would be of no consequence. The expansion zone will interact with the significant quantities of water present in the reactor cavity. Such interaction would cause a large amount of dissipation (condensation) that would help to compensate for the initial expansion trend to sweep away (expel) water from the cavity area. Such dissipation would tend to interfere, in fact, with the fuel dispersal process away from the reactor cavity and into the containment. These processes cannot be evaluated with any degree of certainty at this time. However, the amounts of fuel thus removed would appear to be marginal ($< 10\%$) and such evaluations are not crucial to the remaining of the sequence.

For the in-vessel explosion the inertia constraint is present as well as an essentially one-dimensional shotgun geometry. Clean fluid–solid impacts, on the other hand, may be excluded in view of all the internal solid structures and the expectation that liquid slug breakup, due to its short length, would occur well prior to impact. Even neglecting such uncertain-to-estimate mitigating aspects, however, the explosion energies estimated (few hundred MJ) are essentially one order lower than the many thousands of Mega-Joules estimated to yield potentially damaging missile generation (WASH-1400 [7]).

In conclusion, the steam explosion-induced containment failure probability is judged essentially incredible, i.e., at least two orders-of-magnitude lower than the 10^{-2} estimate given in WASH-1400.

3.5. Needs for future work

With regard to PWR dry containment applications no real needs concerning the energetics aspects of steam explosions appear to exist.

Better understanding the fundamentals would be desirable while large prototypic material experiments offer little progress in this direction.

A short series of prototypic 'intermediate' experiments with *scaled* geometries could also prove useful in shedding some additional light into the 'premixture' questions raised in this study (see also Appendix A).

4. The debris bed coolability concern

4.1. The concern and the approach

Here we are concerned with the character and stability of State D of fig. 3. Current evaluations assume a fast quenching during the transition C → D and the subsequent coolability of the resulting debris bed is then assessed. Taking the whole debri inventory and particle size estimates from small (relatively) scale tests significant uncertainties concerning continued coolability have been raised. Dryout followed by melting and concrete attack has then been assumed followed by computer calculations of containment pressurization due to the release of concrete steam and gases. There are a number of difficulties with this approach:

(a) As has been seen in the previous sections the reactor geometry is not conducive to good mixing. Such fast and complete quenching would be rather improbable (see Appendix A) and even if it were to occur the resulting steam velocity would be high enough to sweep away the cavity water, if not even a good portion of the fuel;

(b) The particle size distributions obtained in available fuel/coolant interaction tests is grossly misleading (too fine) due to important scaling distortions (see Appendix A);

(c) Continued concrete attack by melt in the presence of water can be shown to be an unstable process quickly terminated by fuel freezing as we will demonstrate below.

However, these objections although quite plausible they are quite difficult to conclusively prove. We should resign to the fact, for example, that *we will never know*, nor would it be reasonable to have such an expectation, *the particle size distribution and extent of quenching in state D*. If we ask to calculate, therefore, such things as the steam spike, and bed coolability mechanistically, difficulties due to these uncertainties arise. We will modify the question therefore into a set of questions that are easier to answer now and even quite amenable to confirmatory *prototypic* testing later. The essential feature of this approach is that it converts a 'full scale' problem into a prototypic yet a 'small scale' one. The approach consists of examining *all possible* mechanisms leading into fuel melting and concrete interactions and demonstrating that all such processes are inherently unstable and driven to a stable and coolable configuration. Namely we have to consider the configurations schematically illustrated in fig. 9. In configuration D(a) a separated melt/water system, as it might arise from limited mixing during transition C → D or due to melting on a non-coolable particle bed is depicted. The former may well be the most likely sequence. The melt would attack the concrete the generated gases agitating the melt and bringing about ultimate quenching. The configuration D(b) is characterized by large fuel frozen crusts as might result, for example, by the freezing process of D(a). The resulting bed would be quite penetratable to coolant and stable unless the crust sizes are too large for conducting the decay heat to the surface without substantial melting of the interior. Gradual breakup to stable but still large particle sizes would be expected. Finally, configuration D(c), represents a fully quenched fine particulate bed, rather unlikely to occur (i.e., a rather slow and prolonged transition C → D), but of the type presently often postulated on the basis of available experimental data. For particle sizes less than about 1 mm such a bed would offer great resistance to liquid and vapor flow circulations and [illegible] We will argue that even this situation is unstable since gases from the resulting concrete attack would produce melt sloshing and refreezing on cool particles, and thus a gradual increase in particle size.

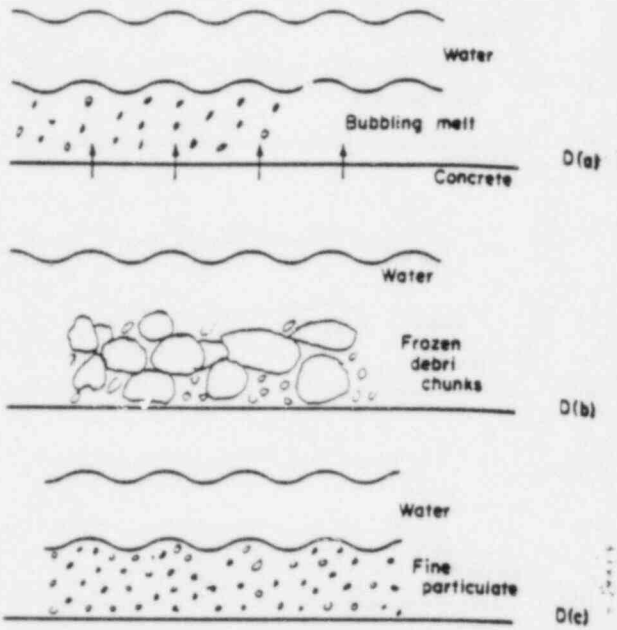

Fig. 9. Illustration of the possible corium-coolant configurations upon the reactor cavity floor (State D).

In summary, then, our approach is based in demonstrating continued coolability for large-particle beds, i.e., sizes greater than a few millimeters and arguing that any deviation from such coolable condition would tend to produce melting and refreezing with a more favorable particle size distribution (stability). Such beds will be referred to as 'coarse' in distinction to those with too 'fine' or too 'chunky' particle length scales. This trend is schematically illustrated in fig. 10. Provided the relevant mechanisms are demonstrated the ultimate outcome is thus completely independent of the details (mixing etc.) of the initial fuel–coolant interaction. In turn all three mentioned mechanisms are quite easy to demonstrate utilizing simulant materials and even prototypic material experiments appear feasible and quite adequate at intermediate scales. Each mechanism is discussed in greater detail in the subsequent three sections but first we will consider the central aspect of the evaluation concerning the coolability of a 'coarse bed.'

Considering a 3000 MWt reactor and a total [illegible] quantity of 150000 kg (100000 kg for fuel and [illegible] and 50000 kg for molten steels, at 1" spec[illegible] the cavity bed would yield a 1 ft depth (assuming porosity) and a surface heat flux of 45 W/cm². On the basis parametric factors such as doubling the decay heat level or artificially restricting debri spreading to the [illegible]

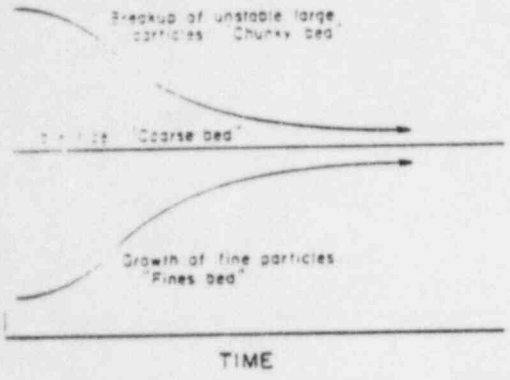

Time-wise evolution (qualitative) of debris particle due to stability considerations.

just beneath the reactor vessel (~ 50% of the total) may be easily scoped by appropriate factors of 2. For our base case *adiabatic* fuel heatup would proceed at ~0.3 K/s and quenching of an all liquid melt to the temperature of 100°C would require heat transfer equivalent to 8000 decay-heat-power-seconds (~ 2.5 hrs). The latent heat of fusion on the other hand would be equivalent to 1500 decay-heat-power-seconds (~ 1/2 hr).

An evaluation of 'coarse' bed coolability may be made with regard to counter-current flow limitations. The flat plate CHF in pool boiling provides one such estimate. Using the Kutateladze (1951) correlation and the properties of interest (with $\rho^* = \rho_l/\rho_v$) we obtain (for water):

$$q_{cr} = 5260\rho^{*-1/2}\ \mathrm{W/cm^2}. \tag{1}$$

Perhaps a more intuitively appealing source may be found in counter-current flow experiments in packed beds (Coulson and Richardson [4]). Based on an earlier correlation by Sherwood flooding data from 16 different gas/liquid pairs in packed towers were correlated in dimensionless coordinates. Considering the inherent variability in this kind of data (i.e., determination of the onset of flooding) the correlation appears successful. In our case the vapor upflow is due to an equal quantity of liquid down flow and for the range of density ratios of interest the flooding data may be simply represented by

$$\frac{j_v^2 a}{g\varepsilon^3}\left[\frac{\mu_l}{\mu_w}\right]^{0.2} = 0.03\rho^{*-1/4} \tag{2}$$

$$\text{for } 100 < \rho^* < 1600.$$

The specific surface area may be expressed in terms of an equivalent sphere diameter and a shape factor to obtain:

$$[\ \ ]\ [\ \ ]$$

For water at 1 bar and a bed with $D_p = 2$ cm and a porosity of 40% this is equivalent to

$$q_{cr} = 5106\rho^{*-1/2}\ \mathrm{W/cm^2}, \tag{4}$$

which is essentially the prediction of eq. (1). The coefficient in eq. (4), contains the $\rho^{*1/4}$ dependence due to casting eq. (3) into the form of eq. (1) for easy comparison. This amounts to a 20% reduction at 5 bar. Further, both equations indicate substantial increase in the critical heat flux with pressure as shown in table 1 for the range of interest.

Also note the relatively strong dependence of eq. (3) on the porosity (see fig. 11). As may be seen in Appendix B porosities of 50% for large irregular particles are not uncommon. The diameter dependence in eq. (3) is rather weak and anyway applications to diameters larger than typical packings (few centimeters) for which the correlation was obtained should be viewed with caution.

Application of these results to a volume-heated debris bed implies that cooling would be available on a continuing basis for the portion of the upper debris bed yielding the predicted amount of surface heat flux. We can clearly see that for 'coarse' beds the predicted performance is well within the heat rejection requirements even including non-currently applied parametric effects on power level and spreading area. Additional safety margins are provided by the following effects:

(a) Actual debri amounts will be less, either due to dispersion in the containment and/or retainment in solid state in the reactor vessel, than the maximum amounts considered here;

(b) The actual decay heat will be less, either due to volatile fission product migration and/or a likely underestimation of the role of coolant (and other heat losses) in the in-vessel portion of the sequence resulting in underestimating the 'cooldown' times;

(c) Grossly asymmetric flows, including two dimensional patterns would be expected to further diminish

Table 1
Counter-current flow limitations

P (bar)	1	2	3	4	5
q_{cr} (W/cm^2)	131	184	228	251	292

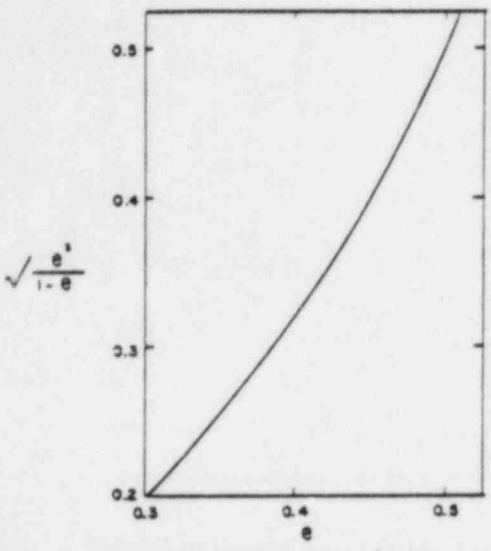

Fig. 11. The porosity group in the critical heat flux eq. (3), as a function of the bed porosity.

the counter-current flow limitations; and

(d) Unsteady bed phenomena including periodic flooding and dryout, coupled with conduction and perhaps even radiation heat transfer mechanisms would favor coolability even further.

The packed bed correlation was obtained from experimental data with columns packed with high voidage, high specific area, packings, such as Rushing rings, saddles, etc. Application to denser particulates, therefore, requires confirmation. A set of experiments, utilizing three different sizes of lead shot and irregular rock fragments was carried out for this purpose with the air/water fluid pair. Details of these experiments are presented in Appendix B. Satisfactory agreement is observed. Initial dryout results for beds with the particle sizes of interest here were also obtained and excellent agreement with predictions of eq. (3) was observed (see Appendix B).

4.2. Large particle breakup mechanisms

At 1% decay heat levels debris particles as large as 1 ft in diameter would survive melting. However, even [illegible] the molten layer, gas mixed, quenching process discussed in section 3.4. It is quite possible that such large chunks will accommodate a molten core either by fully containing the internal stresses (from melt expansion) or, more likely, by gradual relief, i.e., creep of the solid shell into internal porosity, or fine cracking, expulsion of the necessary amount of liquid, and resealing of the crack. More vigorous processes of sudden stress relief and fragmentation of the shell into several pieces with complete exposure of the molten core to the ambient coolant may also be envisioned.

From the point of view, however, of debris coolability all these details are unimportant. The significant aspect is that unstable large chunks will self-destruct into smaller but coarse (and coolable) pieces. Some fine particulate might (in the event of a catastrophic shell failure) be generated in the process however the characteristic size will be of that typical to a quiet quenching in the film boiling regime, i.e., millimeter size rather than the 10–100 micron scale fragments more typical of vigorous interactions.

Scoping experiments were conducted for the purpose of illustrating some of the relevant phenomena. The water/liquid-N_2 fluid pair was selected and microwave heating was utilized to volumetrically heat the water (liquid-N_2 does not couple to microwaves). Simulation of the relevant thermal and mechanical properties of the corium/water system is of course out of the question. Our purpose instead is to explore some of the possible processes and phenomena as a means of thinking and gaining insights for the real system. These experiments are described in Appendix C.

4.3. Small particle growth mechanisms

The dryout mechanism for very fine debris beds (submillimeter sizes) involves strongly two dimensional patterns of liquid down flow and vapor channeling in up flow. The reason is that counter-current flow cannot be accommodated within the extremely small dimensional interstices and channeling and fluidization come into play. Such beds are particularly relevant to fast reactor (LMFBR) conditions due to extensive thermal-stress fragmentation of the fuel coming in contact with the coolant (liquid sodium). A rather strong dependence of the dryout heat flux to particle diameter (to the [illegible] power) is observed here. Since such submillimeter particle beds, although unlikely, cannot be completely ruled out at this time, let us consider the consequences of dryout.

Non-coolable particles will eventually [illegible] forming [illegible] flow pattern due to lifting forces of the gases [illegible] from the melt–concrete interaction. Such slow [illegible] eventually lead to the encounter of completely [illegible] particles and solidification upon them. A gradual [illegible] ing of the particle spectrum distribution to ever larger sizes is thus envisioned, terminating only when

...ving a stably coolable 'coarse' bed. On the other ...d more extensive bed melting and concrete attack. ...ld it occur, would also produce a coolable coarse ...discussed in the next section.

Quenching of a molten layer attacking the concrete

...he key phenomenon here is gas-induced agitation ...f the melt. This process would promote cooling as well ...s prevent the formation of insulating fuel crusts at the interface between the two layers. The process would ...olve again well within the film boiling regime yielding 'coarse' rather than 'fine' solid debris particles.

The phenomena was initially illustrated by means of the liquid-N_2 water/air experiments described in Appendix D. Water was purged by air through a perforated bottom plate in the presence of a superimposed layer of liquid nitrogen. The cooling rates were measured and the freezing characteristics at the extremes of the gas flow rates, corresponding to quiet bubbling, and highly agitated churn-turbulent flow regimes were observed. Indeed at zero gas flows an insulating ice crust quickly forms and the two fluids may remain as such for very long time periods. For the agitated beds the heat fluxes, prior to freezing, were estimated at ~ 7 and ~ 18 W/cm^2 for bubbly and churn flows respectively. These values are one order of magnitude higher than values estimated (using Berenson's correlation) for the film boiling of saturated liquid nitrogen, but do seem to approach the pool boiling CHF limit of 30 W/cm^2. On the other hand the proximity of their values for the clearly stratified, only slightly perturbed, bubbly flow interface, and the clearly violently agitated system seen in the churn flow case indicates that water/nitrogen mixing (at the interface) in the latter case was not as extensive as initially suspected. The temperature gradients within the water were small in both cases. The churn flow experiment was run at superficial gas velocity of 10 cm/s a value typical of concrete attack gas release rates. The bubbly flow at just 1–2 cm/s was carried out to examine the role of mixing intensity in the development of the solidification pattern as well as to simulate the high degree of stratification expected in the corium/water case and feared not to exist at 10 cm/s due to the density proximity of water and liquid nitrogen. Large and coherent but very brittle crusts were formed in both cases. The churning system seemed to freeze throughout the water layer more coherently, as compared to the bubbling one. It is suspected that frozen particles (crystals) tend to coalesce forming the large brittle and porous crusts observed experimentally.

The water/liquid-N_2 system suffered from the proximity of the liquid densities favoring entrainment of one liquid into the other. The anomalous volume expansion of water upon freezing favoring crust flotation at the water–interaction interface was also considered as non-prototypic and undesirable feature. Finally, the rather limited temperature span between the room temperature water and the freezing point limited the precision of the heat transfer coefficient determination at the liquid/liquid bubbling regime. Additional experiments were carried out, therefore, with the Freon-11–liquid-N_2 fluid pair, that yields improvements on all three points mentioned above. With the Freon-11 density 70% greater than that of liquid-N_2 a more definitive stratified regime is possible. Freon-11 crystals are heavier than the liquid and may be observed to rapidly sink in the non-agitated condition. Finally there is a ~ 130°C temperature span between the room temperature Freon-11 and its freezing point, that substantially improves the determination of heat transfer coefficients. These experiments confirmed the trend that as sparging velocity increases an asymptotic limit corresponding to the pool boiling CHF heat flux is reached. In fact the limit was attained at a gas velocity of 10 cm/s and was clearly evident up to the maximum velocity of 16 cm/s utilized. These experiments also revealed certain important aspects of crust formation and positioning. The individually denser (than the liquid) Freon crystals tended to merge forming, just as in the case of water, porous and hence lighter (and floating) crusts. However the tendency for plugging was substantially reduced in comparison to the water/liquid-N_2 system. A more detailed account for these results is given in Appendix E.

Let us now consider the corium–water system. Assuming as a minimum, 1–2 ft of water on the top of the fuel layer in the cavity, an area of ~ 49 ft^2 is available for steam venting. At the limit of entrainment and film-type flooding of 26 m/s (Kutateladze's correlation with $K = 3.68$) we estimate a maximum venting of 7.15×10^4 g/s or the equivalent of 143 MJ/s, or a 317 W/cm^2 heat flux over the 4.5×10^5 cm^2 reactor cavity floor area. (Clearly, the molten layer in this case will spread over the whole available floor areas.) If the rate of initial quenching is greater than this amount cavity water will be entrained and expelled. We see, therefore, that the rate of quenching is self-limiting as discussed earlier. On the other hand a quenching rate less than this amount will not interfere significantly with water existing in the cavity and/or draining back, through the keyway from the containment. With the excellent gas agitation we expect quenching to be limited by countercurrent flow of water and steam. Initially, little penetration into the melt is expected. As the surface layers of

broken up crust are formed penetration of the water deeper into this region is expected. As discussed above the pool boiling CHF would characterize heat transfer under these conditions and from the estimates shown in table 1 we project maximum fluxes in the 200–300 W/cm^2 range depending upon the pressure conditions. Note that these fluxes correspond to more than 100 cm/s vapor velocities, hence the 10 cm/s gas flows would have a negligible influence in these flux estimates. Measurements in gas-bubble-agitated (at 1 cm/s) industrial (100 ton) steel furnaces have yielded heat transfer coefficients of ~ 0.1 W/cm^2 K at the steel/slag interface. This value would be significantly higher for the range of gas velocities expected from concrete decomposition. The heat flux to the upper corium layers, say being completely quenched to the boiling water temperature ($\Delta T = 2200°C$), would be well in excess of 220 W/cm^2. That is, the bed cools uniformly, rather than cooling only near the top layers with the melt persisting at the base. These expected 200–300 W/cm^2 fluxes approach but are well below the 317 W/cm^2 limit established above. The corresponding time to completely quench (accounting for the continuously added 1% decay heat) is estimated (for 250 W/cm^2) at $\sim$ 2222 s that is $\sim O(1/2)$ hr. We note that the time constant of 2 and 4 cm fuel particles is 93 and 372 s that is particle-internal heat transfer is not likely to be limiting over the whole process.

From another point of view the water/melt interface may be assumed, at least initially, blanketed by film boiling. A heat flux of 46 W/cm^2 is estimated using Berenson's correlation. Due to the turbulence at the interface an augmentation by several times this value is easily envisioned. In our nitrogen/water experiments augmentation by one order-of-magnitude was observed. Due to the sensitivity of the film boiling process to the gas thermal conductivity, the fuel/water system is characterized by much higher film boiling heat transfer compared to the cryogenic system. The relative augmentation by interface agitation would be expected to be less, therefore, for the fuel/water case. An upper bound, should, however, be provided by the pool boiling CHF limit. This limit is low for nitrogen (due to the small value of the latent heat of vaporization) and the agitation augmentation in our experiments already yields values up to this limit. For the fuel/water case the CHF limit is quite high but still a factor of four to five augmentation of the [illegible] range. [illegible] perfectly reasonable and consistent with our experimental data. A $\sim 1/2$ hr quench time period is, therefore, again estimated.

4.5. Needs for additional work

It would be desirable for all three mechanisms mentioned in the previous three sections be examined in the light of prototypic material experiments. It is very important (see Appendix D), however, especially for the quenching in the stratified state that wall effects be reduced as far as possible by increasing the lateral dimension of the melt. Since not all conditions might be within the experimental state-of-the-art at present simulant material investigations will have to be continued. Furthermore true bed dryout and post-dryout phenomena need be studied for 'coarse' strongly non-uniform (two-dimensional) beds for the purpose of quantifying the suspected additional margins of conservatism.

5. The containment pressure loading

5.1. Energy sources and sinks

Energy sources intrinsically associated with a core melt accident are due to primary coolant, initial stored energy in the core (that was not removed by the coolant) metal/water reactions and decay heat. Other potential sources are due to hydrogen burning and due to concrete attack (including pressurizing gas source). We concluded in earlier chapters that concrete attack is not to be expected at any large scale. Hydrogen presents a serious difficulty, however. The total quantity from radiolysis and from reacting core materials is known and the corresponding energy to be added to that from the intrinsic sources may be easily estimated. Furthermore, for most melt scenarios, the hydrogen release will take place much earlier than, say, gross core melting and penetration of the reactor vessel, hence its effect [illegible] be scoped in conjunction with the release of the primary coolant, the metal/water reactor energy, and possibly stored core energy. It is convenient therefore, to distinguish between a short-term response and a long term response. The short-term containment response would be similar to that carried out in ECCS analysis with the H_2 contributions taken into account and the [illegible] very much affected by the reliability (availab[illegible] sumptions of engineered safety features (espe[illegible] tainment heat removal systems). The lon[illegible] sponse, on the other hand, [illegible] within the melt-down sequence and [illegible] senting the thrust of this report. Thus time per[illegible] therefore, of interest here. This is not to say that h[illegible] gen evolution may be excluded in the long [illegible]

...ne[ ]t least, the initial heatup and meltdown may ...ur in the dry state (complete loss-of-coolant and ...nplete failure of all ECCS systems) and water en... as long as the transition C → D. The ... ...ans of separating out the hydrogen problem as it may ...t be treated into a realm different than that repre...nting the focus of this work.

Specifically, we are interested in the so-called 'steam ...ke' associated with the rapid quenching of the corium ...elt and the role of passive containment heat sinks in ...e pressure response. The subsequent transient due to ...lease of decay power will also be considered.

In this decoupled approach it is more natural to ...ink of the heat source in terms of a more or less ...ncentrated component associated with quenching the ...rium melt to the containment water temperature (i.e., ...is contains the portion of the initially stored and ...ecay heat energies not already released to the contain...ent) and a distributed component due to decay heat ...nd taken at 1% of rated power. For the total available ...ebri quantities at around the fuel melting point we ...stimate 200000 MJ of stored energy. At 30 MW of ...ecay heat this represents approximately two hours of ...ecay heat. Based on the conclusions of this report, we ...ould expect quenching and release of this energy at a ...uch shorter time period (see previous section). The ...ontributions of these two components may thus be ...valuated separately.

The passive heat sinks consist of a total of 1.62×10^5 ft^2 of 1/4 inch steel (counting the 3.4×10^4 ft^2 at 1/2 ...nch thickness). The total concrete mass in and around ...ontainment is estimated at 4.54×10^5 ft^3. Active sys...ems include sprays and the ECCS heat exchangers ...which most likely have already succeeded in cooling ...down the short-term transient, and fan-coolers which ...again helped cool down the containment prior to the ...long term events considered here. The ECCS heat ex...changers and fancoolers are capable of removing ap...proximately 1 and 4 times the 1% decay power respec...tively. This large capability even if partially impaired ...would be sufficient to cool down the containment atmo...sphere following the primary release of energy and ...hence decouple the response from the long term.

The availability (or not) of power and compounded ...failures in these systems need nevertheless be consid...ered from a reliability-risk perspective. The long time ...periods associated with both the 'short term' (many ...hours) and the 'long term'(days) responses need be ...taken into account in these evaluations such that the ...overall efficacy of various system combinations (includ...ing possibly passive systems) may be adequately judged. Such evaluations, however, are outside the scope of this work.

5.2. The steam spike and subsequent pressure transient

Rather detailed calculations taking into account fragmentation and quenching characteristics as well as condensation heat losses are possible and necessary to calculate the precise containment pressure transient. However, the results are highly dependent on fragmentation size and heat transfer coefficients (noncondensable effects, etc.) assumed and as a result such calculations have been presented as source of justification for more detailed modeling of these complex processes. Our position here is that consideration of such details are distracting from the real issues and that the problem is more easily assessed at a different but more appropriate level of detail consistent with uncertainties inherent to the overall picture.

Let us consider a containment pressurized at ~60 psia with a steam partial pressure of ~40 psia. We calculate the distribution of energy, as proportions of the total quench energy available. For a 2×10^6 ft^3 volume, we estimate 87.5% required for the steam energy exerting the 40 psi in the containment, only 3% is required for heating up the containment air. The time constant for heating the steel liner is only a few seconds and if all came to equilibrium from pre-accident temperatures a 17% portion (33600 MJ) of the quench energy would be required. The concrete sink of the containment shell is at 3.5 and 4.5 ft thicknesses. That internal to containment is 1 ft thick. This concrete has very poor conduction properties and is expected to heat up very slowly. During the 1/2 hour required for the release of the quench energy a thermal boundary layer thickness of 6 cm, *at most*, has developed. The thermal energy stored in this boundary layer is 83000 MJ and represents ~41% of the quench energy. For a 2 million cubic feet containment and the conditions of interest we estimate a pressure-to-energy sensitivity of 4000 MJ/psi. The steel and concrete sinks are, therefore, worth ~8 and ~20 psi respectively. The total heat flux would be 814 J/cm^2 and an average flux during this 1/2 hour would be 0.45 W/cm^2. For an 'average' temperature driving force of 45°C we obtain a heat transfer coefficient of 10^{-2} W/cm^2 K. Even in the presence of air this is a rather modest value considering the high flow rates and turbulence expected, however, the air gap (taken as 0.1 cm) between the concrete and liner has the much smaller heat transfer coefficient of ~$3\ 10^{-3}$ W/cm^2 K and could be of controlling significance. This and other uncertainties including preheating of these sinks during

the previous portion of the accident suggest that not all these indicated *maximum* values of the heat sink benefits may be actually realized.

Based on the above estimates we conclude that the passive heat sinks are of no real significance. For an already cooled containment a 60 psi pressure is predicted soon following vessel meltthrough. The actual time scale for this pressure rise is really immaterial, but based on our earlier discussions would be expected to be more than several minutes. Active containment cooling systems will quickly remove this energy as well as the continuously released decay heat yielding containment depressurization. In case of 100% availability, for example, less than 1 hour would be required for this purpose.

At the other extreme of complete unavailability of these active systems, the quench energy would be released into an already pressurized and heated containment, typically at ~60 psi. Pressurization to about 100 psia following melt quench would now be expected. The sink effects amount to ±20% of this value. If the containment does not fail immediately with the assumed absence of containment cooling failure will soon occur. Other inbetween cases may be considered in a similar fashion, however, it is easy to conclude that our results would be largely independent upon the details of the quench process and the details of heat sink-associated heat transfer coefficients. In fact such details would be completely shadowed by uncertainties in our assumptions concerning availability of the heat removal systems.

It is suggested therefore that major emphasis be placed in assuring operation of containment heat removal systems.

5.3. Needs for additional work

The reliability of containment heat removal systems needs to examined at such level of detail that (a) mechanistic and common mode failures be clearly elucidated, (b) procedures for enhancing reliability due to the long demand periods (allowing for trouble shooting), and the methodology for accounting for such in risk assessment studies, may be established, and (c) the additional safety margins due to augmentation by passive systems may be evaluated.

6. Conclusions

The phenomenology of core-melt accidents in dry containments was examined for the purpose of identifying the margins of safety in such Class-9 situations.

The scale (geometry) effects appear to ultimately limit the extent (severity) of steam explosions. This together with the established reduced explosivity of the corium-A/water system, and the inherently high capability of dry containments (reinforced concrete, and shields in some cases, seismic design etc.) lead to the conclusion that failure due to steam explosions may be considered essentially incredible. These 'premixture' scaling considerations also impact ultimate debris disposition and coolability and need additional development.

A water-flooded reactor cavity would have beneficial effects in limiting (but not necessarily eliminating) melt-concrete interactions. Independently of the initial degree of quenching and/or scale of fragmentation, mechanisms exit that drive the system towards ultimate stability (coolability). Additional studies, with intermediate-scale prototypic materials are recommended to better explore these mechanisms.

Containment heat removal systems must provide the crucial capability of mitigating such accidents. Passive systems should be explored and assessed against currently available and/or improved active systems taking into account the rather loose time constraints required for activation.

It appears that containment margins for accommodating the hydrogen problem are very limited. This problem appears to stand out not only in terms of potential consequences but also in terms of lack of any readily available and clear cut solutions at this time.

Appendix A. Premixture scaling considerations

Even the largest, prototypic material, fuel-coolant interaction experiments available to date are severely limited in providing an adequate base for assessing the outcome and consequences of such interactions at full scale. The reason is that all these experiments are conducted without any consideration for the factors that may exert a non-prototypic influence upon the mixing scale(s) and distribution of the melt into the receiving volume of coolant. These factors in turn will affect not only the quantities potentially participating in the sustaining, and fine, intermixing (energetic fuel-coolant explosions), but also will determine the initial degree of quenching and the associate phenomena of [illegible] (or particle size distribution of solidified [illegible]), (c) entrainment and removal of fuel and/or [illegible] from within the reactor cavity to the outside and melt restratification upon the reactor cavity floor [illegible]

[illegible] attack. As an example, consider the currently [illegible] TS test series at Sandia. A melt volume of [illegible] dumped into 226 l of water. That represents a fuel [illegible] coolant volume ratio of ∼ 1 : 500 (for the two [illegible] scale series this ratio was 1 : 700 and [illegible] to values of ∼ 1 : 2 to ∼ 1 : 4 [illegible] scale (see figs. 1 and 2). The actual [illegible] distortion with respect to the prototype is [illegible] illustrated in fig. A.1. In addition config[illegible] involves a fuel volume scale down (from the proto[illegible] of 1 : 20 000!

T[illegible] expressed purpose of these prototypic material tests [illegible] to determine the 'explosivity' of reactor materials (including the effect of externally applied triggers). In fact, [illegible] conversion efficiencies and particle size distribition of the quenched debri have been utilized in asses[illegible] consequences in applications intended for licens[illegible] considerations. At this point an interesting dilemma arises. On the one hand in view of the enormous scale-up involved and the geometric model distortions mentioned above the empirical and direct application of these data to full core geometries must be viewed with doubt. In the absence of relevant scaling studies we would not even know whether geometric similarity would provide an adequate first approximation nor would we know how to geometrically or materially distort the experiments to correctly simulate the size effect. On the other hand, however, we must also admit that the full understanding of the scaling laws for this kind of mixing problem does not appear to be exactly a trivial task. How is the available experimental information to be, if at all, utilized then? And if no such use can be extracted

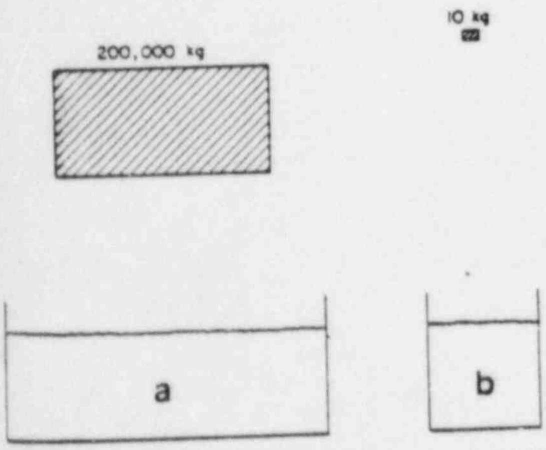

Fig. A.1. Schematic of the melt/water/dropping distance relative scales in the prototype (a) and current intermediate scale experiments (b). The scale-up (based on fuel mass) from the experiment is by 20 000.

what would constitute an alternative experimental basis? It is the purpose of this section to address in a preliminary fashion these questions. In conjunction with this effort we have carried out a number of different experiments. These experiments are not, at this stage, intended to provide a complete data base, but rather a means of demonstrating some [illegible] consider crucial.

In the absence of vapor explosions the mixing process would be rather benign, dominated by film boiling and low transient pressures. It is expected that the benign nature of this process would be self-regulated by the tendency to cut-off (or reduce) further mixing by vapor relief through the 'reactor cavity' water. This water will impose negligible constraint for the time scales characteristic of the relevant heat exchange process here, and would tend to be expelled away from any location where mixing has progressed to any significant degree. We conclude that the process will be driven by the hydrodynamics. We can take a closer look at these fluid–fluid mechanical interactions with the help of the schematic of fig. A.2. The initial state of the melt is shown in a geometrically scaled fashion in relation to the initial configuration of the reactor cavity water including the cylindrical volume just underneath the reactor vessel, to be referred to as 'vessel cavity,' and the tunnel-like, essentially reactangular volume referred to as 'cavity keyway.' The final state of the melt will, of course, be a stratified one (with respect to the water) and is illustrated in two possible configurations although, clearly, other distributions are, as we will see, possible. We will consider that the initial and final states communicate through a jet of diameter (characteristic dimension) d_j. All possible modes of lower head failure (from a small breech to catastrophic failure) may be accommodated by varying the jet diameter up to the size of the initial melt diameter, d_{ir}. Note however that this limit in reality cannot be approached since the jet in this case would arrive within the solid lower heat shield. Mixing between the melt and water, due to the large density difference and hence propensity for separation (stratification) would be a highly dynamic, short lived, phenomenon depending primarily upon the hydrodynamic interaction between the jet and the 'vessel cavity' water. It is convenient to visualize this interaction in terms of its several components.

Upon impact with the 'vessel cavity' floor the jet will be deflected into the horizontal direction. This horizontal motion, in the form of an essentially planar radially outward jet will continue until impact upon the 'vessel cavity' side walls turning the jet once more into the vertical (but now upward) direction. Fall back from this

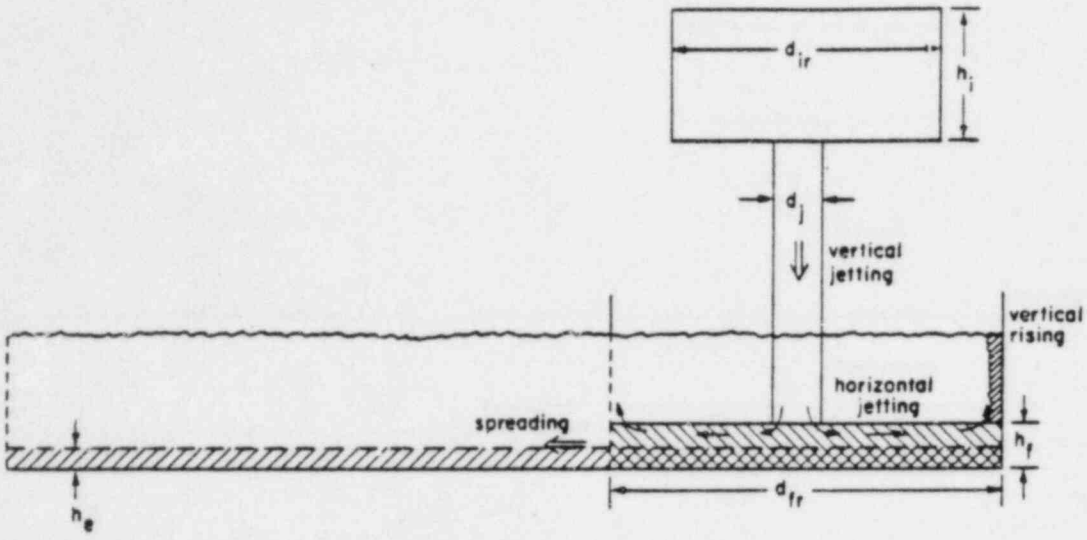

Fig. A.2. Flow patterns and final states in the C → D transition.

position would yield the finally expected stratified configuration. Escape (and spreading) into the 'cavity keyway' would occur (if still in the liquid state) at this time, although a small portion of melt has already escaped by encountering the passage in the horizontally jetting phase. Corresponding to this phenomenology we may identify the following successive phases: vertical jetting, vertical rising, fallback, and spreading. Surface instabilities, in each one of these phases would yield breakup and intermixing. Gravitational settling, on the other hand, would promote separation. The relative importance of these competing factors would vary among the various phases and would depend strongly upon the actual size of the jet.

Let us first consider the case of a small jet diameter ($d_j \to 0$). Clearly the jet will break into droplets well before it reaches the water surface. Additional breakup would occur during the fall through the water mass. There will be a small enough but non-zero value of d_j such that complete quenching of the melt has occurred prior to arriving at the 'vessel cavity' floor. The resulting dispersed and solidified jet could not be deflected into the horizontal direction by the cavity floor and in this limit the debris particles would tend to pile up just under the jet position. As the jet diameter becomes larger (as is to be expected by flow-augmented melting of the flow-path structures) an increasingly larger proportion of the flow will arrive at the floor in the liquid state. hence as the diameter increases the successive phases of horizontal jetting and vertical rising will gradually appear and develop. Neglecting drag forces we estimate jetting velocities of the order of 5–10 m/s. For the vertical jet such velocities imply rather high Reynolds numbers (i.e., 6×10^6 for $d_j \sim 30$ cm). However, the turbulence level in the absence of walls would remain undeveloped and the breakup due to turbulence action on the jet surface should be minimal. That is, an internally (jet) driven breakup mechanism, similar to that found in atomizing nozzles is absent. Potential flow oscillations of the jet as a whole (leading to pinching of whole segments) and surface instabilities (i.e., wave entrainment) remain as likely modes of breakup. The first mode has been investigated theoretically by Rayleigh and the results have been confirmed experimentally, but typically for small size jets found in industrial chemical processes. The most unstable wavelength is 4.5 times the jet diameter and the resulting drops have a size twice the jet diameter. For such large scale instabilities at least three to four wavelengths, that is 13.5 to 18 diameters, would be required for breakup. We conclude that only jets of less than 1 ft in diameter could possibly be subjected to this type of breakup within the travel distances available. It should also be noted that although the original Rayleigh [illegible] ignored the inertia of the surrounding medium, [illegible] analyses took this effect into account [illegible] from small diameter (0.5 cm) jet experiments [illegible] that much larger breakup lengths, than those discussed above are required. Extrapolation of these results to case would yield breakup lengths of $\sim 200d_j$ and $\sim$ [illegible] for turbulent and laminar jets respectively. The [illegible]

[illegible] jets with $d_j \sim 1$ ft not only will break into [illegible] size $2d$ but the drops in turn will break as [illegible] into successive generations of smaller [illegible] would be controlled by [illegible] forces and would be characterized by a [illegible] not too different from that of the initial [illegible] process. As the drops diminish in size so [illegible] the period of oscillations, i.e., faster breakup, [illegible] surface tension and body forces will dominate [illegible] breakup. This final region is characterized by the [illegible] length, l, as initially introduced by Bond to characterize stability of a dispersed phase and later found extensive use in a multiplicity of problems in [illegible] dispersions.

$$l = [\sigma/g(\Delta\rho)]^{1/2} \tag{A.1}$$

The period of oscillations of a spherical drop, in this final capillary region has been given by Rayleigh as

$$\tau = 2\pi(\rho R^3/8\sigma)^{1/2}. \tag{A.2}$$

For a fuel drop with radius of the order of the capillary length (~ 1 cm) we estimate a period of $\tau \sim 0.2$ s. This period would increase rapidly as the drop size increases. This period is to be contrasted to a total travel time of ~ 1 second (at 5 m/s) in order to appreciate that simply there isn't enough time for complete breakup (i.e., to the capillary length size) for jets of order of 1 ft in diameter. We are able hence to define a maximum diameter for complete breakup of ~ 10 cm. Incomplete breakup in the sense outlined above is envisioned for $10 < d_j < 30$ cm. For $d_j \gg 1$ ft Rayleigh breakup would not be expected. Hence surface instabilities (entrainment) need only be examined. Steen's criterion for entrainment in parallel flow

$$\frac{U_f \mu_g}{\sigma_f}\left(\frac{\rho}{\rho_f}\right)^{1/2} > 2.46\ 10^{-4} \tag{A.3}$$

yields a fuel–water relative velocity of ~ 1 m/s, assuming fuel–water contact takes place and $\sim 10^3$ m/s assuming fuel–vapor contact. No information appears to exist for the multiphase multiregion conditions of interest here. However, we note that water contacting the fuel actually implies fuel surface solidification (i.e., resisting entrainment) and taking into account again the short contact times and the lubricating effect of an entrainment and vaporizing surface layer (i.e., decrease of both viscosity and density in the above equation) we conclude that for such jets minimum mixing would be expected in the vertical as well as in the horizontal orientation.

The dynamics of the initial jet-water encounter (impact) remains to be considered. The jet arrives with a dynamic pressure of ~ 5 bar. Depending on the manner in which the breech is initiated the initial quantities of melt will arrive more or less broken up by Taylor and other instabilities. At this point we have effect the greatest amount of mixing and even perhaps heat exchange. Due to the large jet momentum, however, sideways relief would take place, rather than pressure-induced breakup in the unsubmerged portion. In addition the initial tendency of the leading edge would be to produce a vortex ball entraining surrounding fluid as it penetrates the water depth. This type of entrainment is limited in extent and furthermore would tend to be moderated by vapor bubbles occupying the major volume just ahead of the jet leading edge.

As the jet diameter approaches that of the initial melt dimension these initial impact phenomena become increasingly more difficult to quantify. As we have seen earlier such large diameters would correspond to catastrophic lower head failure which would be expected to occur circumferentially and thus yield a melt fall 'shielded' by the accompanying fall of the whole lower head. Nevertheless, 'unshielded' coherent falls are of interest in scoping out the phenomenology of the initial impact.

A number of small scale simulant experiments were carried out. The water/liquid nitrogen system was selected to simulate the fuel/water system of interest. This system is attractive from the point of view of simulating the low intensity of thermal interactions. From the point of view of mixing behavior the two fluid densities are of primary importance. These densities are much closer in the simulation than in the prototype, hence we expect a bias in the simulation for higher mixing and slower separation. In fact solidified water particles will usually be suspended in the highly agitated boiling liquid nitrogen system, such that a convenient method for determining small scale mixing consists of determining the amount of ice found immediately following the interaction. On the other hand the rate of heat transfer between the two liquids will be much higher in the fuel/water case (film boiling coefficient, temperature differences and radiation heat transfer are all greater). Considering these limitations these tests should be viewed as illustrations rather than actual simulations.

First we carried out simple pour experiments of various quantities(3, 10, 100, 1000 cm^3) of water into a large volume of liquid nitrogen. These pours were manually carried out from a height of 10 cm above the nitrogen and no particular effort for speed was made. The small jet regime discussed earlier would be ex-

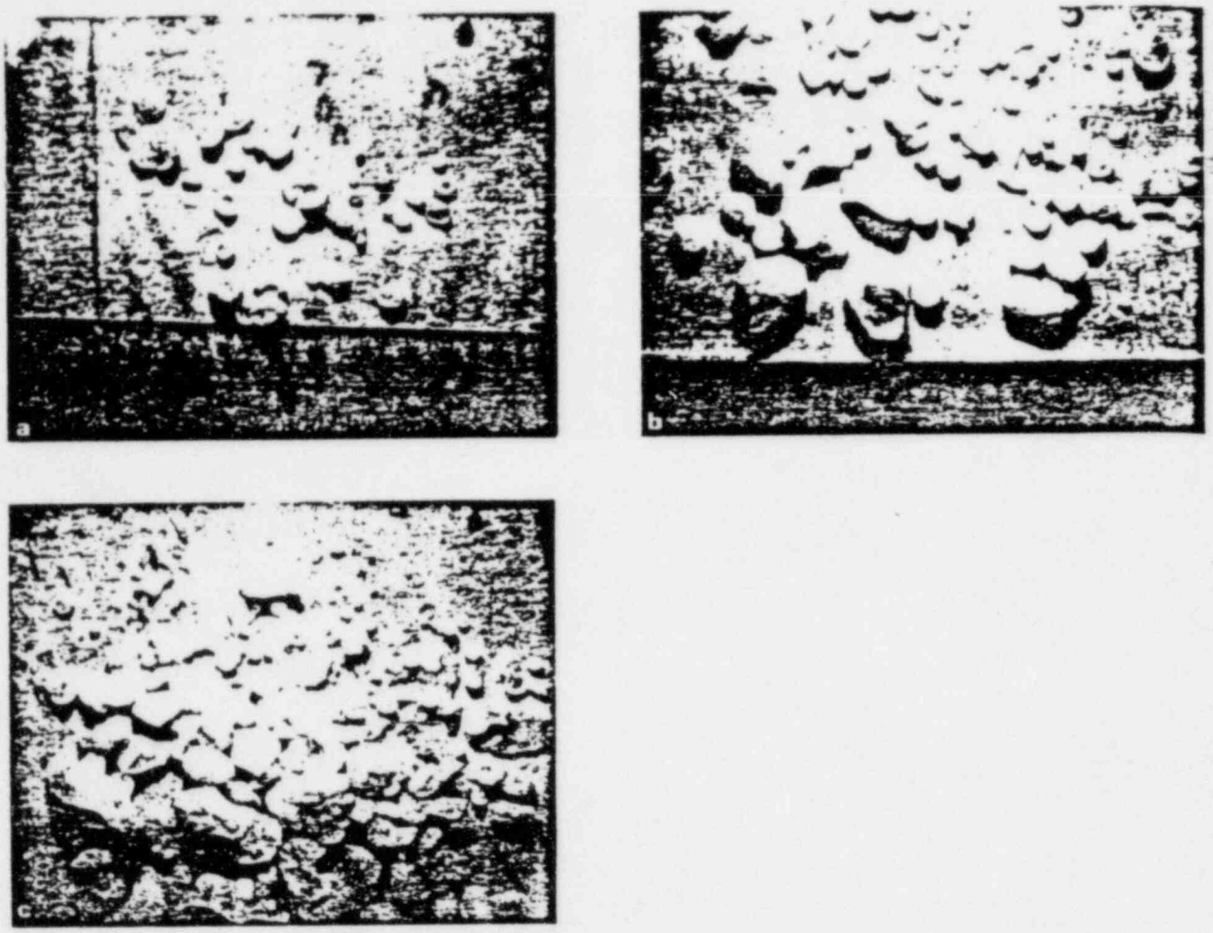

Fig. A.3. Solidified water (debris) formations from the pouring of (a) 3 cm³, (b) 10 cm³, (c) 100 cm³, (d) 1000 cm³ of water into a pool of liquid N_2. Note the large sizes and smooth surfaces indicative of freezing in film boiling. Particle agglomeration in irregularly shaped, porous crusts is seen in the large water pours. Such crust are brittle and disintegrate by handling (e).

...ed. Indeed, all water was frozen into spherical par... typical of solidification in the film boiling regime. ... geometric dimensions and resulting ice ... cm and most particle sizes are of this ...

...fferent pours were carried out in the experimental ...paratus shown in fig. A.4. Geometric similarity with ... vessel cavity' and initial melt configuration per fig. ...2 was observed. 'Melt' volumes of 5 l and 0.5 l were employed. the water volume was held in an inverted cylindrical container with the help of vacuum and was sealed in the cylindrical segment by two free, thin, semicircular plexiglas segments eliminating surface instabilities. Release of the vacuum produced free fall of the water volume and simultaneous displacement of the plexiglas segments (supported on their side) to the side. The water mass was observed (with the help of television records) to undergo all phases of penetration and deflections mentioned above. The initially frozen mass was measured either by withdrawing an already submerged screen mesh immediately following the interaction (1–2 seconds) or by pouring the whole contents through a screen mesh immediately following the interaction (4–8 seconds) with good agreement in results. The total water quantity was also measured and by difference the amount expelled due to entrainment in the nitrogen vapor flow was found. The results are summarized in table A.1.

We note that the very small proportion of the mass (~2–4%) frozen. The expelled mass appears to be the order of ~20%. This amount appears to indicate some aspects of the self-limiting interaction characteristics discussed above, since both the frozen as well as the expelled mass proportions are judged small relative to the rather large degree of dispersion observed in the

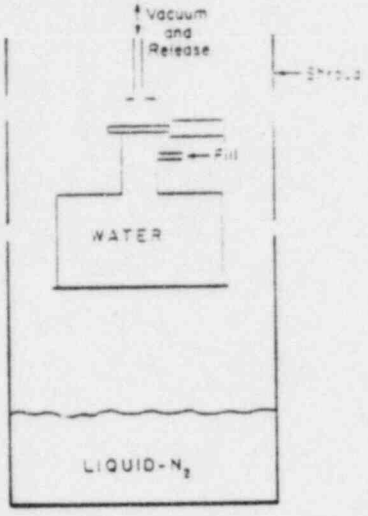

Fig. A.4. Schematic of the experimental apparatus for coherent pours of water into liquid-N_2.

leading edge of the descending water volume. Again we emphasize that such carry-over would not be typical in the densities and velocities of the prototype. Even so, however, these experiments do support the idea that the major portion of the melt would collapse unquenched at the cavity floor.

Appendix B. Counter-current flow limitations in coarse beds

The counter-current flow of air and water was studied in the apparatus shown in fig. B.1. The steady state water and air flow rates were measured for lead shot beds with particles 2, 4.2, and 12.6 mm as well as for

Table A.1.
Results of coherent water pours in liquid-N_2

Run number	total water volume (l)	% Frozen	% Remaining as liquid	% Entrained
5	5	2	76	22
6	5	3	79	18
7	5	4	76	20
17*	5	3.4	68	28.6
18	5	2.4	82	15.6
14	0.5	~0	88	12
15	0.5	~0	90	10
16	0.5	~0	84	16

* Dropping distance increased by 25 cm.

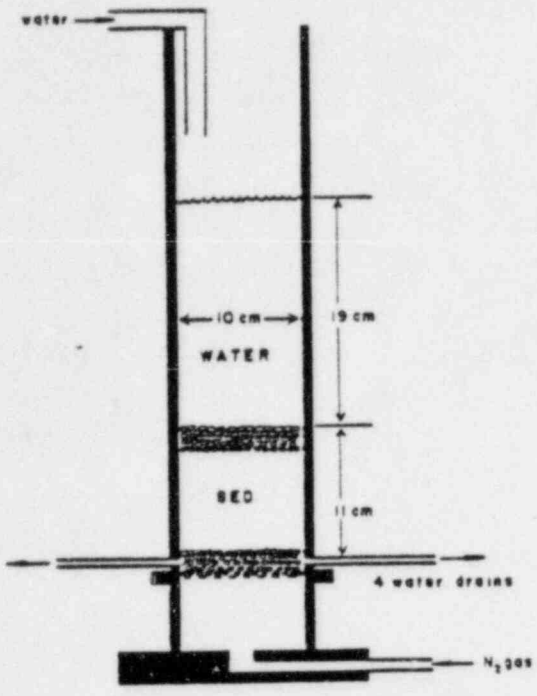

Fig. B.1. Schematic of the experimental apparatus used in two-component packed bed counter-current flow tests.

Fig. B.2. Rock particulate and the three lead shot sizes used in the two-component packed bed counter-current flow tests.

one rock material particulate of characteristic dimension similar to that of the large lead shot dimension. The actual shapes of the rock particulate is shown in fig. B.2. The same bed depth of 11 cm was utilized in all cases. Water layer was maintained to the quantity equivalent to a collapsed dimension of 19 cm as shown in fig. B.1. For each nitrogen flow setting determination of the liquid downflow, at steady-state, was made.

The experimental results are presented in figs. B.3–B.6. The condition of interest for dryout of heated beds is when the liquid downflow exactly matches the gas upflow. The gas velocities corresponding to this critical condition are compared to the 'predictions' of section 4.1 in fig. B.7. For the small size range good agreement with eq. (2) is observed. For the large particles the prediction becomes increasingly conservative. It is possible that wall effects begin to become evident for a vessel-to-particle diameter ratio of less than 10. Such nonuniformity effects are very important for the actual application expected in fact to exhibit gross spatial non-

in non-heated two-component experiments and have not been reported even for heated bed experiments. We are in the process of investigating this matter. This qualification, however, is considered only as a matter of completeness since even if certain portions of the bed are not as well irrigated (or even dried out) water availability to the bed bottom would insure ultimate cooling by flooding from below.

A preliminary series of dryout experiments with deep, coarse, particulate beds were also carried out and the results are presented here. Coarse, rocky, particulates of three different sizes (see fig. B.8) were volumetrically heated using a 5 kw microwave oven facility. Freon-11

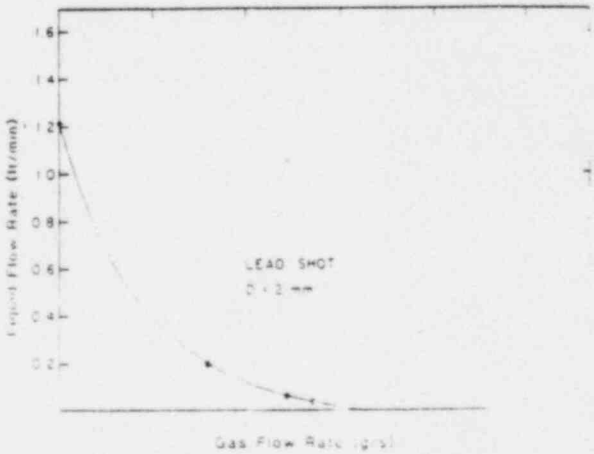

Fig. B.3. Experimental data for the counter-current f water and nitrogen in a packed bed of 2 mm lead sh Porosity $\epsilon = 0.43$.

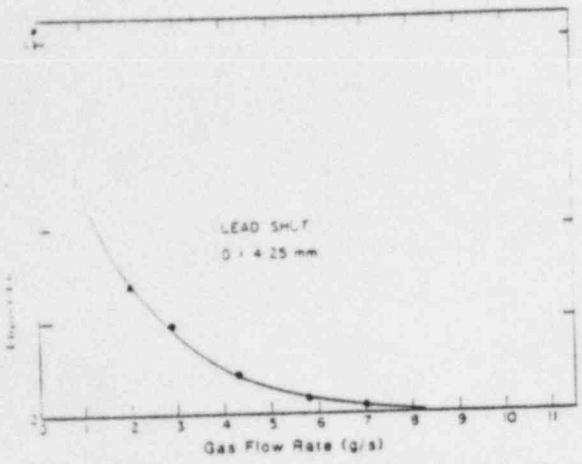

Fig. B.4. Experimental data for the counter-current flow of water and nitrogen in a packed bed of 4.25 mm lead shot particles. Porosity e = 0.45.

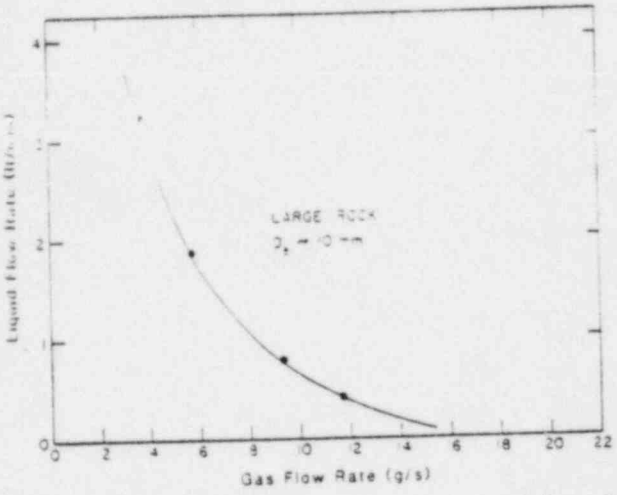

Fig. B.6. Experimental data for the counter-current flow of water and nitrogen in a packed bed of 10 mm rock particles. Porosity e = 0.5.

was utilized as the coolant. Dryout was detected by noting the melting of color-coded wax (crayons) particles or small polyethylene particles imbedded at regular, one-inch axial intervals along the bed centerline. Four different size (10.5, 9.5, 8.5 and 8 cm ID) cylindrical test sections with a bed depth of 30 cm were utilized. The bed porosities were around 50% and slightly increased from 0.47 for the small size to 0.51 for the large size particles. Experiments were initiated from a fully flooded condition. Power was slowly increased to the full level and maintained at a steady level for at least 5 minutes. We estimate ~40 seconds to vaporize the interstitial Freon in the bed locations, near the bottom that will ultimately dryout and calibrations indicate that the crayons or polyethylene particles will melt within 1-1.5 minutes in a dry bed. Liquid Freon was continuously supplied to maintain the two-phase level near the top of the test section (~30 cm of the two-phase layer). Through calibrations of the coupling efficiency for the

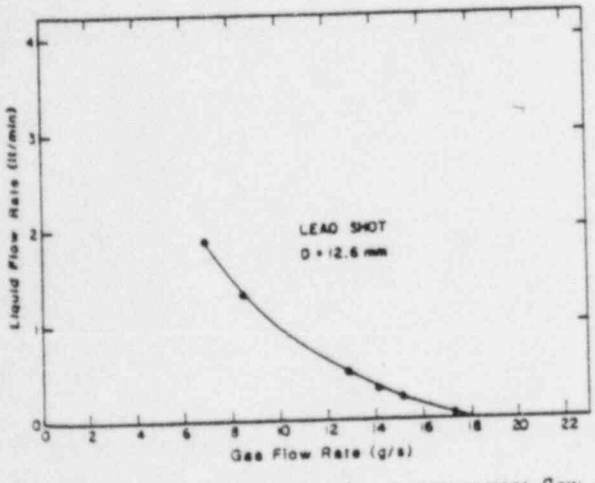

Fig. B.5. Experimental data for the counter-current flow of water and nitrogen in a packed bed of 12.6 mm lead shot particles. Porosity e = 0.47.

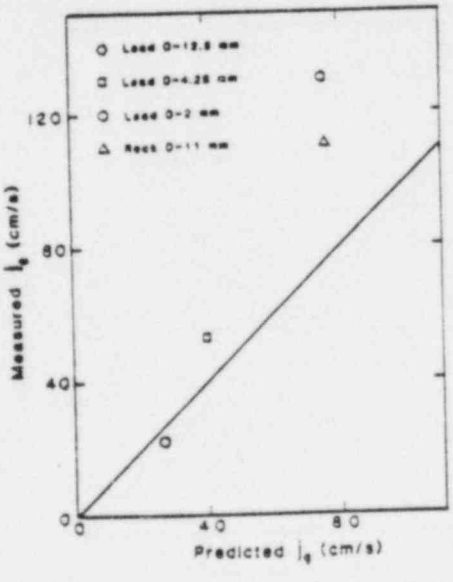

Fig. B.7. Comparison of experimental nitrogen superficial velocities at the "critical condition" with the predictions of eq. (2).

Fig. B.8. The three sizes of rock particulate utilized in the bed dryout studies.

dry bed and the fluid (slight absorption) the operating heat flux for each experiment could be determined. From the resulting height of the dryout region the dryout heat flux could be determined.

Operating fluxes up to 52 W/cm^2 were obtained. The pool boiling critical heat flux for Freon-11, eq. (1), is ~ 30 cm^2. The dryout heat fluxes measured are compared to those predicted by eq. (3) in fig. B.9. A shape factor of $F = 1.5$ was utilized in these predictions. The equivalent particle diameter was found by measuring the mean particle volume from 100 randomly selected

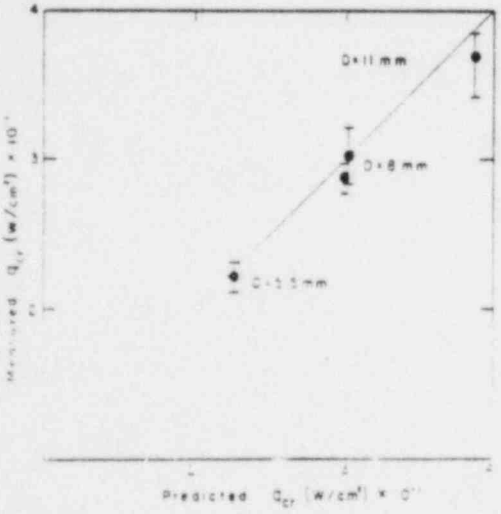

Fig. B.9. Comparison of measured dryout fluxes with those predicted using eq. (3).

particles, for each bed. Satisfactory overall agreement is observed. For the large particles the wall effects seem to begin to become important (particle-to-cylinder diameter ration $\sim 1:8$). Liquid bypassing the bed along the cylindrical test section wall could be observed over the whole height. This liquid kept the bottom 1-inch of the bed wetted, however, the next three inches up were dried out. Larger-in-diameter beds would be more appropriate for testing this particle size, however, the present oven power rating does not allow this test.

Appendix C. Large particle breakup behavior

In considering the stability of large fuel particles subjected to the combined effects of decay heating in the volume and water cooling at the surface we must be concerned with a number of possible configurations. The simplest, and the one commonly discussed, is a solid sphere (or similar shape) with its maximum (center) temperature just below the melting point of fuel. The idea is that this is the maximum possible stable size since any larger size would yield phase change in the center, associated internal stresses and rupture into smaller (and stable) fragments. It is reasonable to expect that this type of consideration would be correct but only in an order-of-magnitude sense since the actual response of such an oversized particle would depend on a number of other important factors not taken into account in the simple concept stated above. Such factors must include the solid crust mechanical properties and the actual mechanics of breakup (or simply cracking) and stress relief mechanisms. Even so a number of interesting questions arise in connection with establishing the actual morphology of the solidified debri. For example, how do such particles at, or above, the critical size form under the continuous influence of the decay heat or should the maximum expected particle size be limited *at formation* by the critical size? And if unstable particles indeed form how do they breakup and what is the resulting particulate dimensions? Unless disintegration of the major portion of the unstable chunks to the submillimeter (fine) particle range was to occur, which is clearly incredible, these details are not [illegible] for the conclusions of practical interest here [illegible] term bed coolability). The problem is discussed [illegible] in terms of competition

[illegible] cooled by boiling water is a 29 cm in diameter [illegible] For water heated volumetrically at the same [illegible] density and cooled by boiling liquid nitrogen the [illegible] size is a 9 cm in diameter sphere (i.e., 0.26 l [illegible]

...tion to the good simulation characteristics of this ...er system from the point of view of film boiling and ...losive characteristics, as discussed in section 3.2 ...tion for the problem at hand. In fact the temperature gradients are quite close also, i.e., ~150°C/cm versus 50°C/cm for the fuel and water system respectively. The thermal expansion coefficient of water is ... above difference and yielding similar stress behavior.

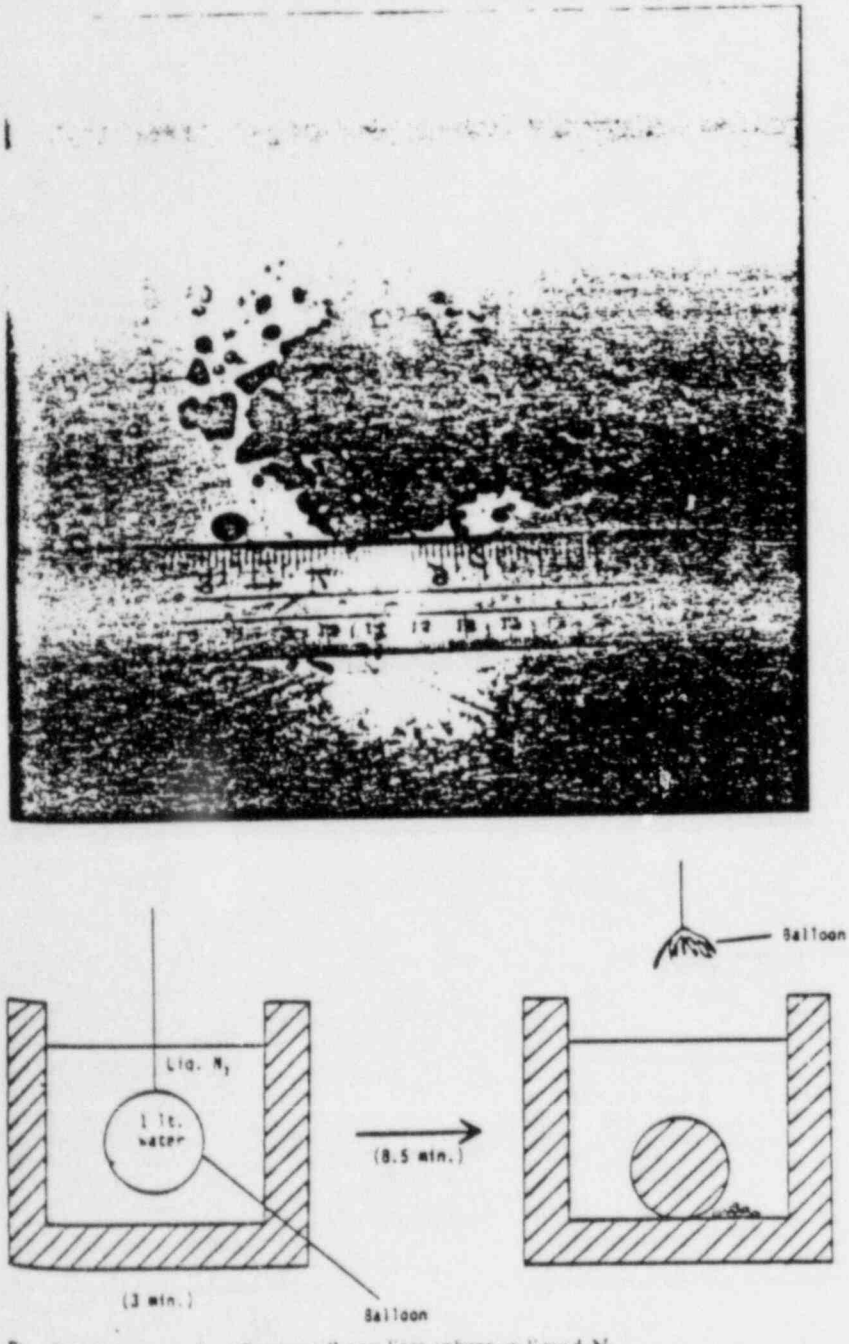

Fig. C.1. Behavior of a "3-minute" one-liter sphere in liquid-N_2.

The anomalous expansion characteristics of water around the freezing point is also noted to emphasize that the intent here is not to exactly simulate but rather to assure similar overall regimes and gain some insights into the possible ranges of phenomenology. That is we are interested in the fragmentation behavior of frozen

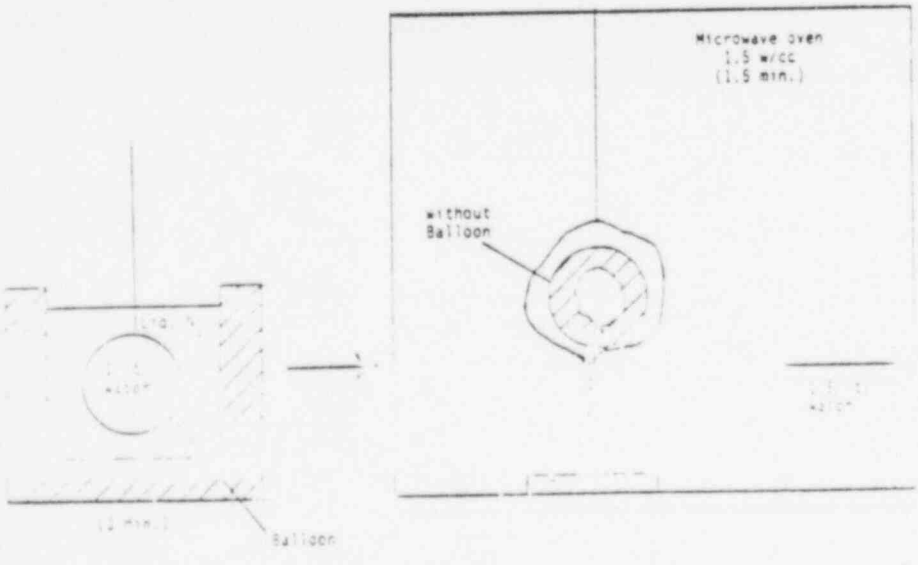

Fig. 6.2. Response of a suspended 3-minute sphere to 1.5 minutes of microwave heating at 1.5 w/cm

...(C5) and the expulsion of their liquid contents) due ... thermal stresses produced not only as a result of solid ... liquid phase change but also due to cooling-induced ... stresses. Volumetric heating was accomplished ...

... microwave oven. Water possesses excellent microwave coupling properties all the way to freezing temperatures, however, a discontinuity occurs upon freezing, such that the ice remains essentially uncoupled. Our samples consisted, therefore, of partially frozen spheres, i.e., containing a liquid core of known quantity, and in many cases colored, such that we can identify the origin of fragments following breakup. The experiments progressed through several stages of calibrations and trials and the results are presented in that sequence below.

One- and two-liter ice spheres were produced by immersing water-filled balloons into liquid nitrogen. A submergence of ~3 minutes produced rather stable, partially, but symetrically, frozen spheres with a shell thickness of 2 cm. Such spheres will henceforth be referred to as '3-minute' spheres, and are found to contain a 0.3 l liquid core (for 1 l case). If the freezing process was allowed to continue often a small amount (~20 cc) of "coarse" ice particulate was created. The large ice sphere itself bore no signs of fragmentation, except for 'mended' surface scars. It appears that internal stresses due to volume expansion upon freezing cause *cracking* of the frozen crust, small amount of liquid expulsion which yields the particulates and upon stress relief quick refreezing and thus mending of the cell crack. Fig. C.1 indicates the phenomenology for a ... sphere ...

... a still air environment ... fountaining of ice cubes) where the expelled liquid jet is subcooled and freezes as it is expelled upwards forming an inverted stalactite. This phenomenon is even more pronounced in the case of two-liter spheres giving rise to substantially larger amounts of particulate.

A microwave power calibration was carried out by suspending an 1 l 3-minute sphere into the microwave oven and irradiating at 1.5 W/cc. After 1 minute a leak developed at the lower side followed by complete draining of the liquid core. The remaining hollow shell, following an additional 30 seconds of irradiation is shown in fig. C.2. Next, a similar 3-minute sphere was irradiated at the same power density, but while fully immersed in liquid nitrogen. At ~8.5 minutes sudden activity was noticed with copious nitrogen vaporization and audible boiling noises (fig. C.3). A ruptured hollow shell (bulging around the ruptured area) and 120 cm^3 equivalent volume of *coarse* ice particulate, both shown in fig. C.4 resulted. An additional portion of water (not accounted in the 120 cm^3 of particulate) is frozen around the shell rupture area such that at least, if not more, the initially present water amount was expelled. Several similar experiments confirmed these general trends.

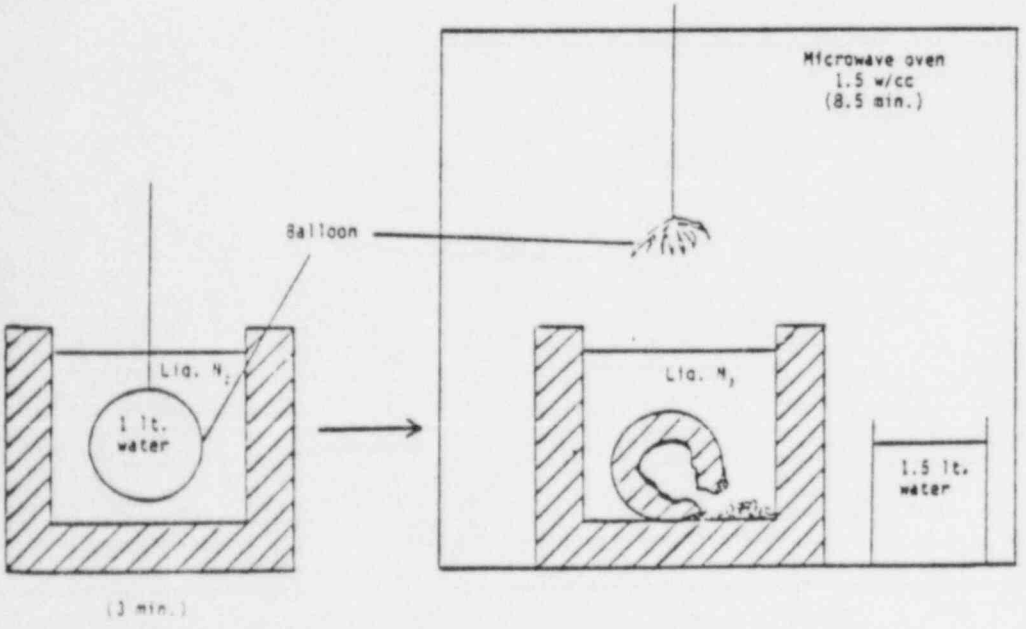

Fig. C.3 Response of a submerged 3-minute sphere to 8.5 minutes of 1.5 w/cm^3 microwave irradiation.

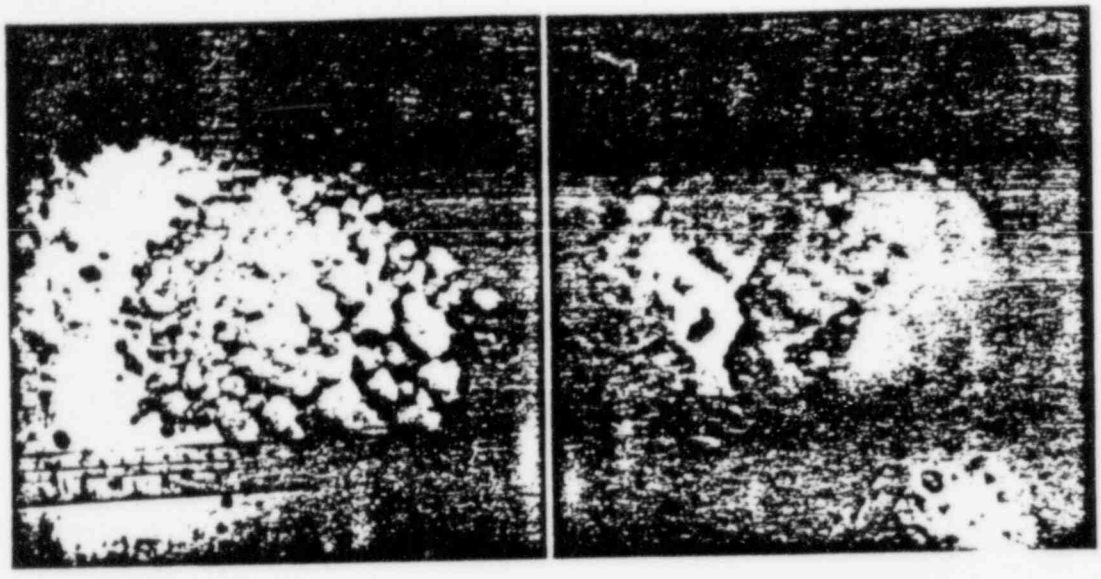

Fig. C.4. Illustration of "rupture" and the resulting particulate from the processshown in fig. C.3.

Fuel chunks of size greater than the critical size are not impossible, in fact as discussed in Appendix D they are even likely, on a temporary basis. Quenching under highly agitated conditions may yield, for example, agglomeration of particles stuck together by liquid films. The films are due to liquid sloshing amidst a solidified particulate suspension. In the final stages of this ever thickening fluidized (by gases) slurry local particulate conditions may reach well subfreezing temperatures such that they may serve as freezing substrates for any liquid coming in contact when in close proximity 'welding' of more than one particle (or chunk) together can be expected. Similarly, such welding may be taking place rapidly enough, such that an amount of liquid becomes totally enclosed in a frozen shell yielding a chunk (with a liquid core) of size much greater than the critical size is also possible. Subsequently a wide range of possible beavior may be envisaged also. From a totally contained internal melt (porosity, strong shells), to a gradual relief and limited relief (cracking, limited expansion, remending of cracks), to substantial expulsion and creation of empty shells and course particulate. Our experiments demonstrate the possibility of this latter behavior, perhaps the one most difficult to visualize and to expect

'aerated' by 5–10 cm/s gas flow due to concrete attack by the melt. Again the water/liquid nitrogen system is utilized. The nitrogen does not couple to the microwaves and a simulation including the decay heat effects could be carried out in the microwave oven. However, radiation heat losses cannot be matched and the convection (boiling) heat transfer mechanisms are not understood well to allow a choice for the 'simulant' power level. Furthermore we found it necessary to work with quantities of 'fuel' in excess of 10 l in order to avoid an important size effect and for such quantities it would appear that the available oven power is inadequate. However, the available cooling is much greater than the decay power level and is expected to dominate. Hence the consideration of the uncoupled problem does not entail a major compromise.

In the absence of agitation by the gas bubbles, an insulating ice crust, at the interface between the two liquids quickly forms and this liquid–liquid configuration remains stable for a very long time. In the process of decay heating a 1 ft melt layer cooled only from above would never freeze completely. We expected that agitation would breakup this insulating crust [illegible]

Appendix D. Quenching in the stratified state

Here we would like to consider the quenching characteristics of a layer of corium melt, $L \sim 30$ cm, and

Our initial experiments were conducted in a [illegible] diameter plexiglas cylinder utilizing an 30 cm water layer flooded with an equal volume of liquid nitrogen. The cylinder bottom was perforated such that nitrogen

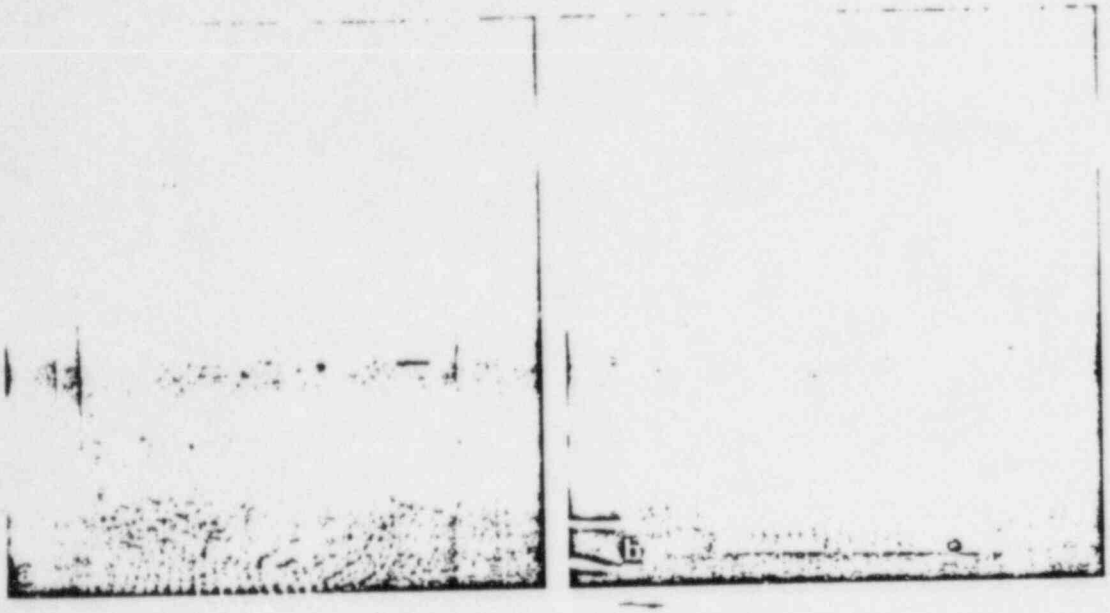

Fig. D.1. Flow regimes in water sparged by gas at (a) ~1 cm/s and (b) 10 cm/s.

gas could be injected at measured and controlled rates. Superficial velocities of 10 cm/s were utilized and the expected churn-turbulent flow regime was observed. The whole water layer cooled rather rapidly and ice formation proceeded at high rates starting at the liquid/liquid interface. The ice did not form as a simple, thin, insulating layer as the one found in the absence of agitation, but rather as a collection of highly contorted irregular shaped chunks. Each chunk turned out to be rather porous and brittle and appeared to consist of a conglomeration of smaller particles. However this process quickly formed a plug (~7 cm thick) sealing off the gas flow and thus interrupting the agitation and the whole freezing process. This mechanism

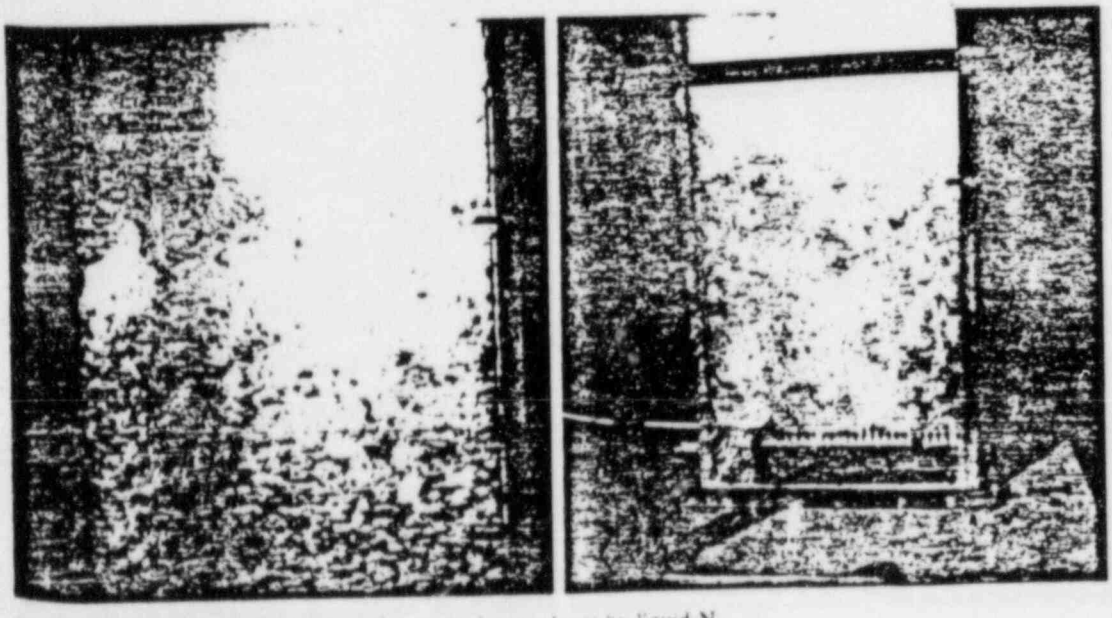

Fig. D.2. The quenching phenomena of a sparged water layer by liquid-N_2.

must be kept particularly in mind as one contemplates similar tests with prototypic materials where quantities must be kept to a convenient but adequate minimum.

Our next series of experiments were carried out in a large rectangular, 30 cm on the side, plexiglas test section. A 30 cm water layer was utilized and an equal amount of liquid nitrogen was maintained on the top. Air injection through the bottom perforated plate was set at 10 cm/s (churn turbulent) in one experiment and at 1 cm/s (bubbly) in the other. In this manner the influence of the degree of interface (liquid/liquid) breakup and interdispersion could be investigated.

This difference and the corresponding two-phase flow regimes may be seen in fig. D.1. The vertical temperature gradient was measured by means of three thermocouples located at the top, center, and bottom of the water layer. The behavior in these experiments was very similar to that observed in the previous cylindrical

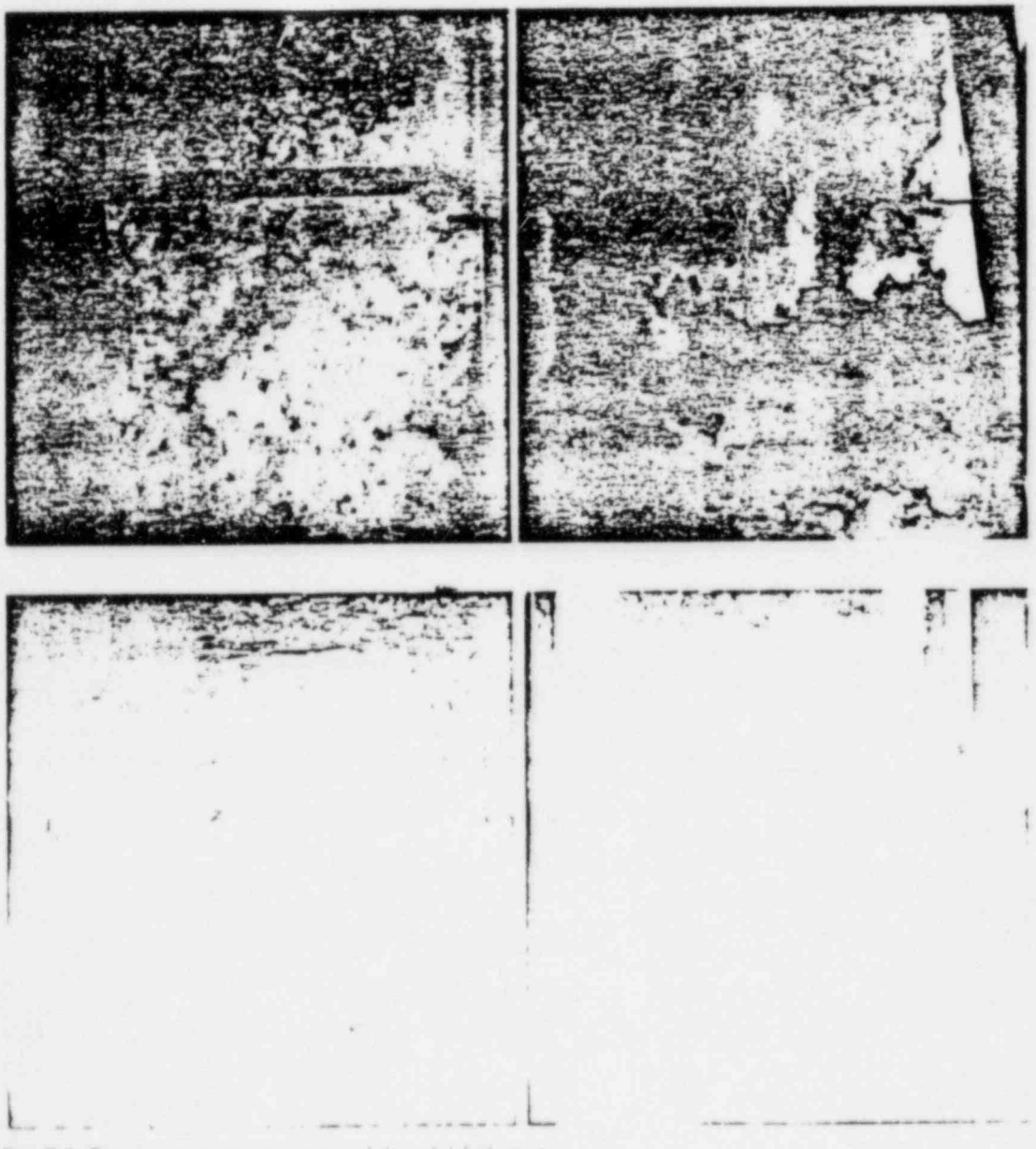

Fig. D.3. The post quench appearance of the solidified crusts.

...ons, however, due to the large cross-section em-...yed now no plugging was observed and the experi-...ts could be carried to completion (complete solidifi-...

...reezing point of water. From this cooldown rate we ...ce heat fluxes of 7 and 18 W/cm² for the 'bubbly' ...'churn' runs respectively. Considering the proximity ...ese values our concern that the intense agitation in ...'churn' experiment and the non-prototypic proxim-...of the densities of the two liquids produced extensive and uncharacteristic dispersion of the two liquids does not appear founded. Once initiated, freezing continued at an accelerated pace. The 'bubbly' run exhibited a downward propagation of the freeze boundary somewhat more distinct than the one observed in the 'churny' run however in both cases the freezing proceeded in a more or less uniform fashion. The resulting ice was porous, irregularly shaped, and rather brittle. Its appearance during the freezing and at the end of the experiment may be seen in figs. D.2 and D.3 respectively. Such large and convoluted crusts with characteristic dimension well into the coarse region should be typical of those expected in prototypic situations.

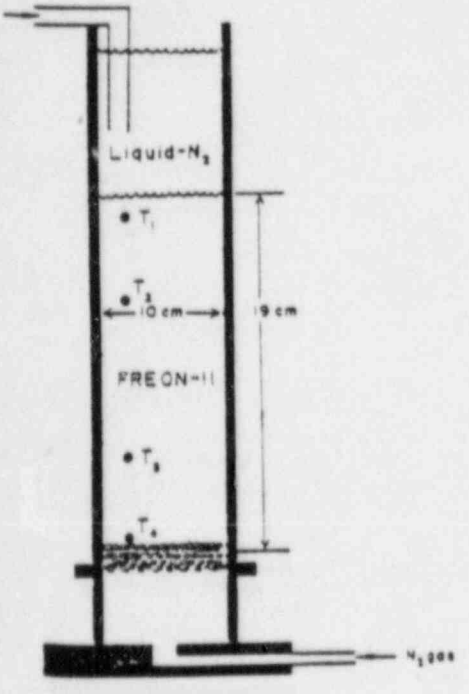

Fig. E.1. Experimental apparatus for the Freon-11/liquid-N_2 liquid/liquid heat transfer tests.

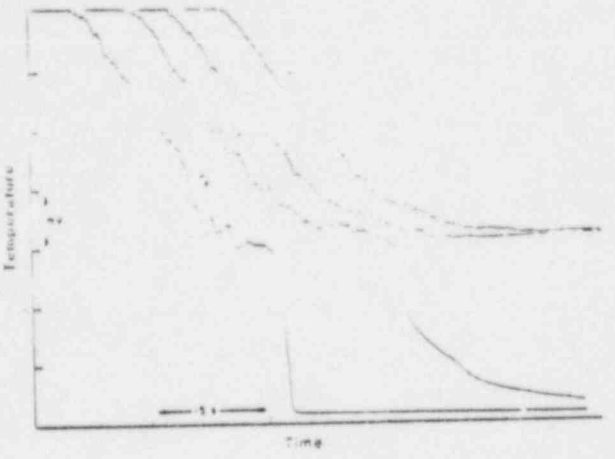

Fig. E.2. Typical temperature transients in a Freon-11 layer quenched by liquid-N_2. Gas velocity: 13.3 cm/s.

Appendix E. Film boiling—liquid/liquid heat transfer in the stratified sparged state

A more detailed investigation of liquid/liquid heat transfer in the gas-sparged, stratified regime was carried out in the apparatus of fig. E.1. The Freon-11 layer was sparged by nitrogen gas and was quenched by the addition of liquid-N_2 at the top. The temperature drop transients yielded clearly defined and steady (for a given gas flow) rate (fig. E.2). These results are summarized in fig. E.3. An asymptotic behavior is noted beyond a gas velocity of 10 cm/s. The measured cooling rate of this limit corresponds to a heat loss of ~ 34.6 W/cm², i.e., a value very close to the pool boiling critical heat flux of

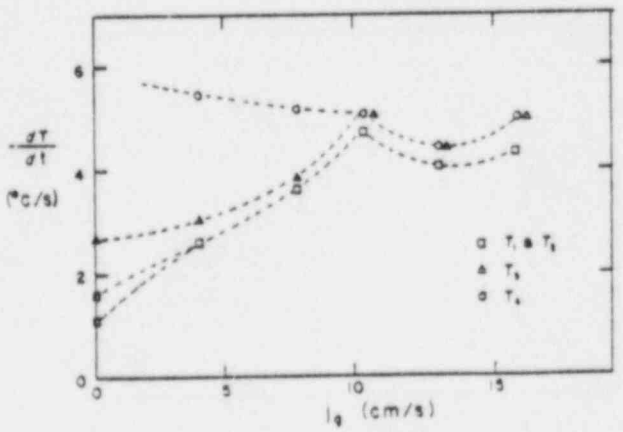

Fig. E.3. Cooling rates at several Freon layer locations (see fig. E.1) as functions of the sparging gas velocity.